

5-15-2019

## A unique role for clathrin light chain A in cell spreading and migration.

Oxana M. Tsygankova  
*Thomas Jefferson University*

James H. Keen  
*Thomas Jefferson University*

Follow this and additional works at: <https://jdc.jefferson.edu/bmpfp>

 Part of the [Medical Biochemistry Commons](#), and the [Medical Cell Biology Commons](#)

[Let us know how access to this document benefits you](#)

---

### Recommended Citation

Tsygankova, Oxana M. and Keen, James H., "A unique role for clathrin light chain A in cell spreading and migration." (2019). *Department of Biochemistry and Molecular Biology Faculty Papers*. Paper 154.

<https://jdc.jefferson.edu/bmpfp/154>

This Article is brought to you for free and open access by the Jefferson Digital Commons. The Jefferson Digital Commons is a service of Thomas Jefferson University's [Center for Teaching and Learning \(CTL\)](#). The Commons is a showcase for Jefferson books and journals, peer-reviewed scholarly publications, unique historical collections from the University archives, and teaching tools. The Jefferson Digital Commons allows researchers and interested readers anywhere in the world to learn about and keep up to date with Jefferson scholarship. This article has been accepted for inclusion in Department of Biochemistry and Molecular Biology Faculty Papers by an authorized administrator of the Jefferson Digital Commons. For more information, please contact: [JeffersonDigitalCommons@jefferson.edu](mailto:JeffersonDigitalCommons@jefferson.edu).

## RESEARCH ARTICLE

# A unique role for clathrin light chain A in cell spreading and migration

Oxana M. Tsygankova and James H. Keen\*

**ABSTRACT**

Clathrin heavy chain is the structural component of the clathrin triskelion, but unique functions for the two distinct and highly conserved clathrin light chains (CLCa and CLCb, also known as CLTA and CLTB, respectively) have been elusive. Here, we show that following detachment and replating, CLCa is uniquely responsible for promoting efficient cell spreading and migration. Selective depletion of CLCa, but not of CLCb, reduced the initial phase of isotropic spreading of HeLa, H1299 and HEK293 cells by 60–80% compared to siRNA controls, and wound closure and motility by ~50%. Surface levels of  $\beta$ 1-integrins were unaffected by CLCa depletion. However, CLCa was required for effective targeting of FAK (also known as PTK2) and paxillin to the adherent surface of spreading cells, for integrin-mediated activation of Src, FAK and paxillin, and for maturation of focal adhesions, but not their microtubule-based turnover. Depletion of CLCa also blocked the interaction of clathrin with the nucleation-promoting factor WAVE complex, and altered actin distribution. Furthermore, preferential recruitment of CLCa to budding protrusions was also observed. These results comprise the first identification of CLCa-specific functions, with implications for normal and neoplastic integrin-based signaling and cell migration.

**KEY WORDS:** Clathrin, Cell spreading, Focal adhesions, Integrin signaling

**INTRODUCTION**

Clathrin has well-established functions in cellular membrane trafficking events. These include mediating endocytosis of diverse cargoes from coated pits in the plasma membrane, sorting of biosynthetic cargoes from coated buds in the *trans*-Golgi network (TGN), and roles in intracellular trafficking pathways from coated tubular and vacuolar domains on sorting endosomes to other compartments in the endolysosomal network (Klumperman and Raposo, 2014; Schreij et al., 2016). In addition, non-canonical roles for clathrin that have been more recently recognized include stabilization of the mitotic spindle in dividing cells (Royle, 2012; Royle et al., 2005), WAVE complex-mediated lamellipodium formation and migration in lymphocytes (Gautier et al., 2011; Ramirez-Santiago et al., 2016), anchorage to collagen fibers in cells migrating in 3D environments (Elkhatib et al., 2017) and others (Brodsky et al., 2014). Given this diversity, understanding the


determinants for clathrin action in these and potentially other novel clathrin functions are important goals.

Clathrin exhibits a high degree of evolutionary conservation, and the protomer is composed of three heavy chains (CHCs) and three light chains (CLCs). The former are ~50% identical between human and yeast (Payne and Schekman, 1985), and their triskelion shape comprises the lattice structure (Keen et al., 1979; Ungewickell and Branton, 1981) that provides a framework for binding of adaptors for cargo recruitment and for contributing to membrane bending (McMahon and Gallop, 2005; Traub and Bonifacio, 2013). A single light chain gene exists in yeast (Silveira et al., 1990), while local gene duplication in the vertebrate lineage (Wakeham et al., 2005) apparently generated two distinct clathrin light chains (a and b, here denoted CLCa and CLCb, also known as CLTA and CLTB, respectively). Mammalian CLCa and CLCb polypeptides are ~60% identical at the amino acid level (Jackson et al., 1987), and both the identical and distinct regions show high degrees of evolutionary conservation as well. This attribute, as well as tissue-specific expression levels of each CLC that are also conserved (Wakeham et al., 2005), suggest that each CLC has unique functions in cells. However, essentially all known functions ascribed to clathrin light chains appear to be shared by both light chains and, where identified, involve identical sequences. These include modulation of *in vitro* clathrin lattice assembly and disassembly (Brodsky, 2012; Schmid et al., 1984; Ungewickell and Ungewickell, 1991), LRRK2 binding and Rac1 inactivation (Schreij et al., 2015), gyrating-clathrin (G-clathrin) formation and cargo recycling (Luo et al., 2013; Majeed et al., 2014; Parachoniak et al., 2011; Zhao and Keen, 2008, and this study), internalization of some G-protein-coupled receptors (GPCRs) (Ferreira et al., 2012; Maib et al., 2018) and Hip1-mediated actin interaction (Chen and Brodsky, 2005; Engqvist-Goldstein et al., 2001; Legendre-Guillemin et al., 2002; Legendre-Guillemin et al., 2005). Recently, a role for CLCb in the modulation of endocytic coated pit dynamics and EGFR processing has been identified (Chen et al., 2017b), and the importance of CLCa for internalization of some GPCRs has been inferred from immunological phenotypes in knockout mice (Wu et al., 2016), validating the concept of CLC-specific functions.

We previously reported that upon interfering with the production of both CLCs in mammalian cells, which does not discernibly affect formation of plasma membrane or TGN clathrin coat structures or the endocytic uptake of most cargoes (Huang et al., 2004; Poupon et al., 2008), the appearance of G-clathrin structures are greatly reduced. These highly dynamic, tubular endosomal structures contribute to recycling of transferrin and its receptor, the growth factor c-Met, and Na/K-ATPase and inactive  $\beta$ 1-integrin; upon CLC depletion, cell migration is also substantially reduced (Majeed et al., 2014; Parachoniak et al., 2011; Zhao and Keen, 2008). In an effort to further dissect the role of CLCs in these processes, we undertook to evaluate effects of depletion of each CLC individually. Surprisingly, we observed that CLCa, but not CLCb, was required

Department of Biochemistry and Molecular Biology, Cell Biology and Signaling Program of the Sidney Kimmel Cancer Center, Thomas Jefferson University, Philadelphia, PA 19107, USA.

\*Author for correspondence (James.keen@jefferson.edu)

 J.H.K., 0000-0003-0753-8690

Received 17 August 2018; Accepted 1 April 2019

for efficient cell spreading after plating on an extracellular matrix (ECM) substrate. We determine that CLCa, but not CLCb, is important for early events in adhesion-activated signaling pathways, targeting of adhesion-related components to the adherent surface of spreading cells, focal adhesion (FA) maturation and cell migration, as assessed by wound closure and motility assays.

## RESULTS

### Depletion of CLCa inhibits cell spreading

To dissect the potential roles of individual CLCs in recycling events, we began by depleting HeLa cells of CLCa and assessing G-clathrin by using YFP-GGA1 as a reporter (Zhao and Keen, 2008). The amount of G-clathrin was unchanged under these conditions compared to controls, but we also noticed that these cells were very slow to spread after plating. As seen in the time-lapse phase-contrast microscopy images in Fig. S1, a much higher proportion of these cells maintained a highly rounded appearance at 2–4 h after plating, while the control cells began spreading effectively within the initial 15–60 min. We then used multiple, well-characterized siRNA constructs to deplete each CLC individually in HeLa cells plated on collagen-IV, as its receptor  $\beta$ 1-integrin is the most prevalent  $\beta$ -integrin in HeLa cells (Riikonen et al., 1995). These results were then compared with those for cells expressing a negative control siRNA (NC). As assayed by immunoblotting after these treatments (Fig. 1), levels of CLCa were routinely decreased by 80–90%, and that of CLCb by closer to 95% compared to controls. Depletion of either CLC alone did not significantly affect CHC levels, as reported previously (Wu et al., 2016). Treatment with either of two CLCa-targeted siRNAs spanning different regions of the human non-neuronal CLCa message and quantification of spreading revealed 70–80% inhibition of HeLa cell spreading at 2 h after replating (Fig. 1A,B), and similar effects were seen in H1299 and HEK293 cells (Fig. 1C,D). Knockdown of CLCb did not inhibit spreading; a slight increase was seen in H1299 and HEK293 cells at 60 min but was not significant thereafter, which may reflect increased CLCa occupancy of clathrin triskelia in the absence of CLCb. We also designed an epitope-tagged siRNA-resistant CLCa construct (designated CLCa-R, see Materials and Methods). When co-transfected into CLCa-depleted HeLa cells, CLCa-R fully rescued the ability of expressing cells to effectively spread following plating (Fig. 1B). These results provide evidence against a role for off-target siRNA effects in the inhibition of spreading, and indicate that CLCa is both necessary and sufficient for efficient spreading after cell detachment and replating.

These findings were extended to ask whether cell migration was also affected by CLCa depletion. In a wound-healing assay using H1299 cells, depletion of CLCa, but not CLCb, resulted in an ~50% decrease in rate of wound closure compared to control cells (Fig. 1E). Finally, we also examined HEK293 cells in a time-lapse imaging motility assay (Fig. 1F). Here too, cells depleted of CLCa showed comparable decreases in cell velocity (~51%) with no significant change in directionality compared to NC cells. Taken together, these results indicate that CLCa, but not CLCb, is critical for cell spreading and subsequent migration in multiple human cell lines.

### Depletion of CLCa does not affect cell attachment or surface integrin levels

Inhibition of spreading and motility in CLCa-depleted cells could be consequences of reduced surface integrin levels, a phenomenon we previously reported in cells simultaneously depleted of both CLCs (Majeed et al., 2014). Surface integrins also mediate initial cell attachment (Huttenlocher and Horwitz, 2011; Wolfenson et al., 2013), so we looked at plating efficiency in cells depleted of either

CLC alone. In both HeLa and H1299 cells, no differences in initial cell attachment were found compared to controls (Fig. S2A). Biochemical measurement of total  $\beta$ 1-integrin levels showed that their levels were unaffected by knockdown of either CLC individually (Fig. S2B). We then quantified surface levels of activated and inactive  $\beta$ 1-integrins separately by performing an intact-cell antibody binding assay. CLCa-depleted and NC cells were fixed and stained with  $\beta$ 1-integrin-conformation-specific antibodies and appropriate secondary antibodies and then assayed by fluorescence-activated cell sorting (FACS) analysis. To quantify the level of activated  $\beta$ 1-integrins, we used antibodies 12G10 or 9EG7, while inactive  $\beta$ 1-integrins were probed using monoclonal antibody (mAb) 13 or 4B4 (Byron et al., 2009). As expected, the majority of cell surface  $\beta$ 1-integrins were in an inactive conformation (Tiwari et al., 2011), and no significant differences for either integrin were found between CLCa-, CLCb-depleted or control samples in HeLa (Fig. S2C), HEK293 and H1299 cells (data not shown). Overall, these results indicate that the continued presence of either CLC is able to support unchanged levels of surface  $\beta$ 1-integrins upon depletion of the other CLC, likely due to persistence of G-clathrin and its contribution to rapid recycling under these conditions. In contrast, simultaneous depletion of both CLCa and CLCb results in an ~60% decrease of inactive surface  $\beta$ 1-integrins as a consequence of inhibition of its recycling (Majeed et al., 2014).

Cell spreading on substrates and subsequent migration has been shown to require internalization and recycling of integrins and other FA components (Alanko et al., 2015; Arjonen et al., 2012; Ezratty et al., 2009; Nader et al., 2016). Accordingly, the possibility remained that surface and internal integrin levels in CLCa-depleted cells might be similar to those in controls, but lack the dynamics necessary to support cell spreading. To investigate this possibility further, we used a fluorescent antibody-based internalization assay to examine the fate of inactive  $\beta$ 1-integrins initially present on the cell surface. In HeLa NC cells imaged immediately after antibody binding in the cold, but before warmup and internalization, labeling of adhesion structures at the adherent surface was observed (Fig. S2D), consistent with the known steady-state distribution of inactive  $\beta$ 1-integrins (Arjonen et al., 2012; Fang et al., 2010). In CLCa-depleted samples, fewer and less-well-defined apparent FAs were present, and more signal was present in smaller, dispersed spots in the cell periphery. However, within 10 min of cells being warmed to 37°C, in both control and CLCa-depleted samples, punctate signals, reflecting an accumulation of internalized  $\beta$ 1-integrins in intracellular endocytic structures, were apparent, and these signals increased at the 30 and 60 min time points (Fig. S2D). Quantification revealed that the levels of internalized anti- $\beta$ 1-integrin Ab were virtually identical in NC and CLCa-depleted [denoted knockdown (KD)-a] cells throughout this period (Fig. S2E); furthermore, essentially all cells in both sample groups showed accumulation of these labeled organelles. To probe recycling dynamics, we also allowed internalization of antibody-labeled  $\beta$ 1-integrin for 30 min and then differentially stained for surface and internal antibody pools. While this assay would not fully distinguish recycled surface  $\beta$ 1-integrin from that which failed to be internalized, the comparable surface labeling in control and KD-a cells (Fig. S3) support the indication that  $\beta$ 1-integrins are dynamic under both conditions. Finally, we also looked at uptake of fluorescently labeled transferrin, a clathrin-mediated endocytosis marker. Again, no significant differences were found between NC and KD-a cells (data not shown), as expected from previous observations showing that CLCs are not required for clathrin-mediated endocytosis

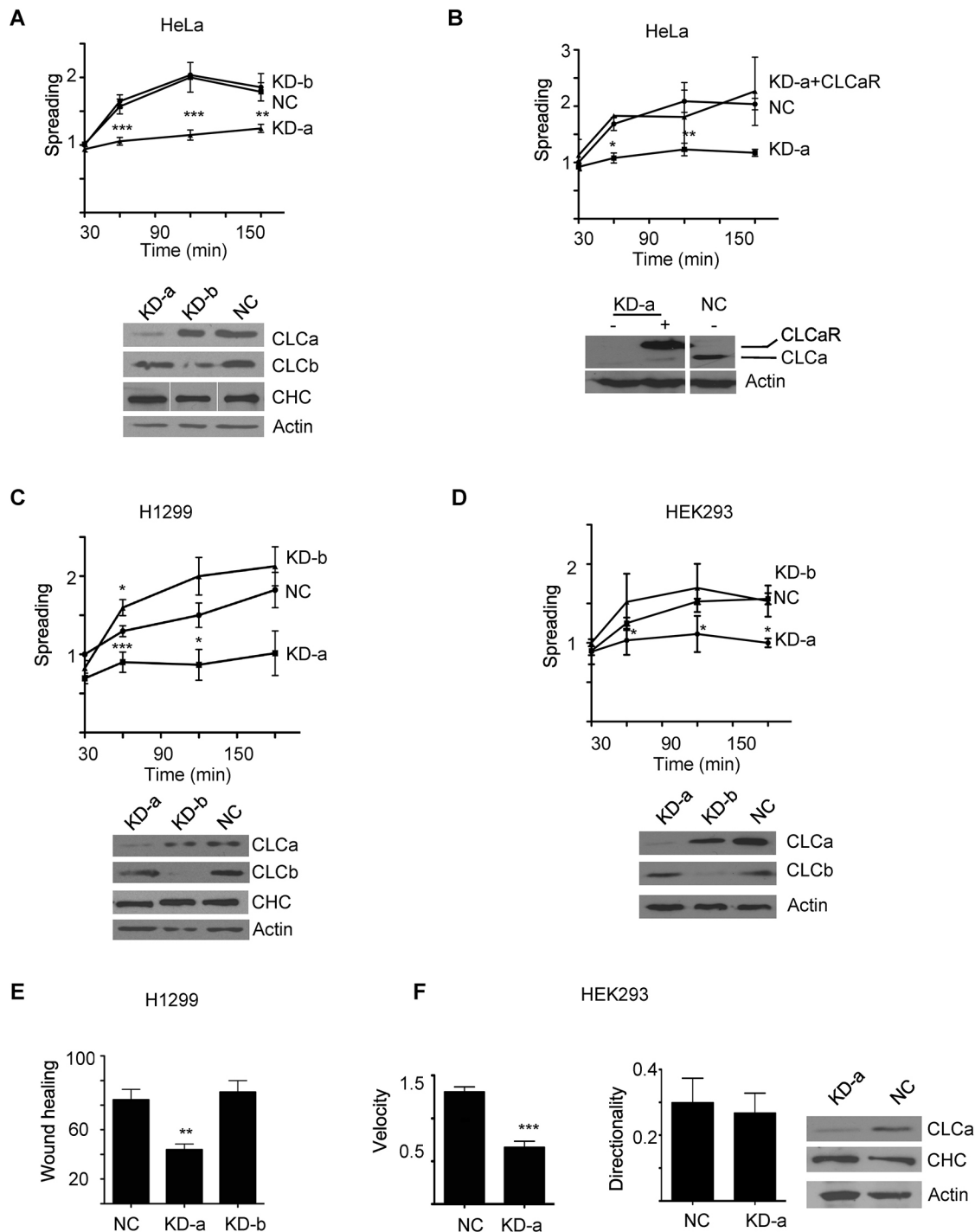


**Fig. 1. Depletion of CLCa, but not CLCb, specifically inhibits cell spreading and motility.** (A) HeLa cells were transiently transfected with Qiagen CLCa (KD-a), CLCb (KD-b) or negative control (NC) siRNAs (see Materials and Methods for details) and analyzed for spreading on collagen IV at indicated time points. Cellular spreading was denoted as fold change over spreading of NC-transfected cells at 30 min. Data from 5–7 plating experiments are summarized together. (B) HeLa cells were transiently transfected with Dharmacon CLCa siRNA with or without siRNA-resistant CLCa DNA (CLCaR) and analyzed for spreading as described for A. (C,D) H1299 and HEK293 cells were transiently transfected with Dharmacon CLCa, Qiagen CLCb or NC siRNAs and analyzed for spreading as described in A. (E) siRNA-transfected H1299 cells were plated on collagen IV-coated dishes and grown to confluence. After scratching three of four wounds per siRNA, cells were allowed to recover for 20 h and analyzed for wound closure. Complete wound healing was set as 100%. The graph represents data from three independent experiments. (F) Velocity and directionality of siRNA-transfected HEK293 cells were analyzed by time-lapse microscopy and ImageJ chemotaxis software. 20–50 cells per siRNA were analyzed in two independent experiments. Western blots are presented as confirmation of knockdown. \* $P < 0.05$ ; \*\* $P < 0.01$ ; \*\*\* $P < 0.001$ .

(Huang et al., 2004; Poupon et al., 2008). Taken together, these results indicate that CLCa-depleted cells maintain dynamic surface pools of  $\beta 1$ -integrins that are comparable to those in control cells.

#### Rac1 activation, actin organization and clathrin-WAVE interaction are inhibited in KD-a cells

Cell spreading following attachment to integrin-activating substrates involves actin-dependent lamellipodial formation, FA maturation,

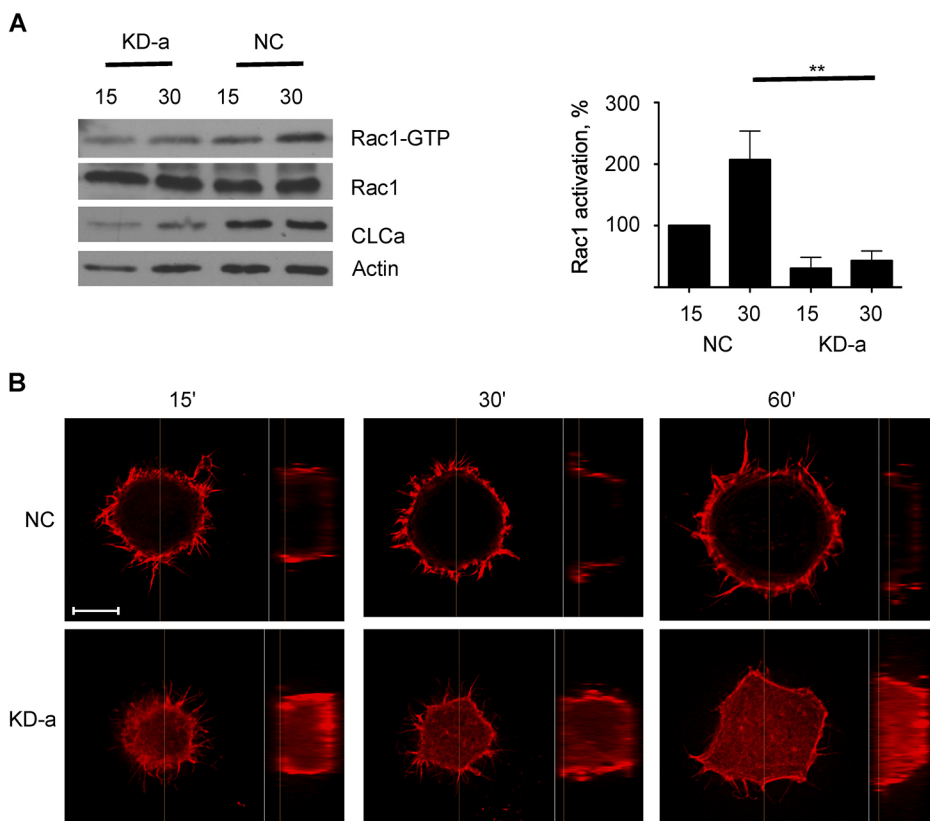


tension development and formation of protrusions. Activation of the small Rho family GTPase Rac (D'Souza-Schorey et al., 1998; Price et al., 1998) and its downstream effectors contribute to these effects through induction of actin rearrangements that drive lamellipodial extension (Herman et al., 1981; Xiong et al., 2010). Using an assay for active GTP-bound Rac1, we found that there was a rapid increase in Rac1-GTP in NC cells at 30 min after plating (Fig. 2A). However, in KD-a cells Rac1 activation was strongly inhibited ( $\geq 80\%$  at 30 min).

We then asked whether actin localization was perturbed in cells depleted of CLCa by visualizing F-actin using fluorescently tagged phalloidin. In control cells imaged at 15 min after plating, actin near the adherent surface was initially present in bundles at the cell periphery, as well as distributed over the plasma membrane surface, as revealed by confocal  $y$ - $z$  sections (Fig. 2B, upper panel). Over the subsequent 30–60 min after plating, F-actin was progressively concentrated at the spreading cell periphery near the adherent surface, while it was largely depleted from the upper regions of the cell (Fig. 2B,  $y$ - $z$  panels). However, in KD-a cells the F-actin distribution was markedly different. At 15 min after plating, a much smaller proportion of cellular actin was organized into bundles present near the adherent surface. At later times, a continuous actin-stained ring could be detected. However, even at these times a much smaller proportion of cellular actin signal was recruited to the bottom adherent surface, while a larger fraction remained on or near the upper plasma membrane. In addition, diffuse phalloidin-stained actin signal was apparent throughout the cytoplasm of KD-a cells, which was virtually absent from NC cells; this staining likely represents short, randomly oriented F-actin filaments or bundles (Fig. 2B). We conclude that inhibited Rac1 activation and failure to effectively organize actin at the adherent surface of KD-a cells contributes to the diminished spreading of CLCa-depleted cells compared to controls.

Biochemical and morphological evidence has been presented for an association of clathrin with WASP-family verprolin homologous protein 2 (WAVE2; also known as WASF2), a component of the Scar/WAVE complex of WASP proteins that regulates Arp2/3-mediated activation of F-actin polymerization in lamellipodia (Gautier et al., 2011; Machesky and Insall, 1998; Miki et al., 1998). These findings and the aberrant distribution of actin in CLCa-depleted cells, as well as the key role played by actin in some forms of clathrin-dependent endocytosis (Collins et al., 2011; Messa et al., 2014; Skruzny et al., 2012), prompted us to investigate the effect of CLC depletion on clathrin–WAVE protein interactions in HeLa cells, which express both WAVE1 and WAVE2 (Bierne et al., 2005). In control cells, immunofluorescence staining for WAVE2 extended to the edge of the cells, where it often colocalized or was in close proximity to fine clathrin staining, in which puncta were noticeably dimmer and smaller in apparent size than more centripetal coat structures, as well as nearby diffuse regions of larger and more irregular shape (Fig. 3A and insets, and see Fig. 8). Clathrin-coated pit staining was also present in KD-a cells, which is expected as both coated pit formation and endocytosis do not require CLCs (Huang et al., 2004; Poupon et al., 2008). However, in these cells the WAVE2 staining had receded from an outer ring of clathrin staining and a substantial separation was now observed between the two proteins. An object-based image segmentation analysis of entire cell volumes made using the Fiji plugin SQUASSH (Rizk et al., 2014) confirmed a highly significant decrease in colocalization upon CLCa depletion (see legend to Fig. 3A).

Given the extensive distribution of both proteins throughout both control and CLCa-depleted cells, we also used a proximity ligation assay (PLA) that reports on loci containing the presence of both antibodies within sub-resolution distances (Gomes et al., 2016; Söderberg et al., 2006). We were limited to using an antibody to CHC (herein referring to CLTC) reported to bind near the



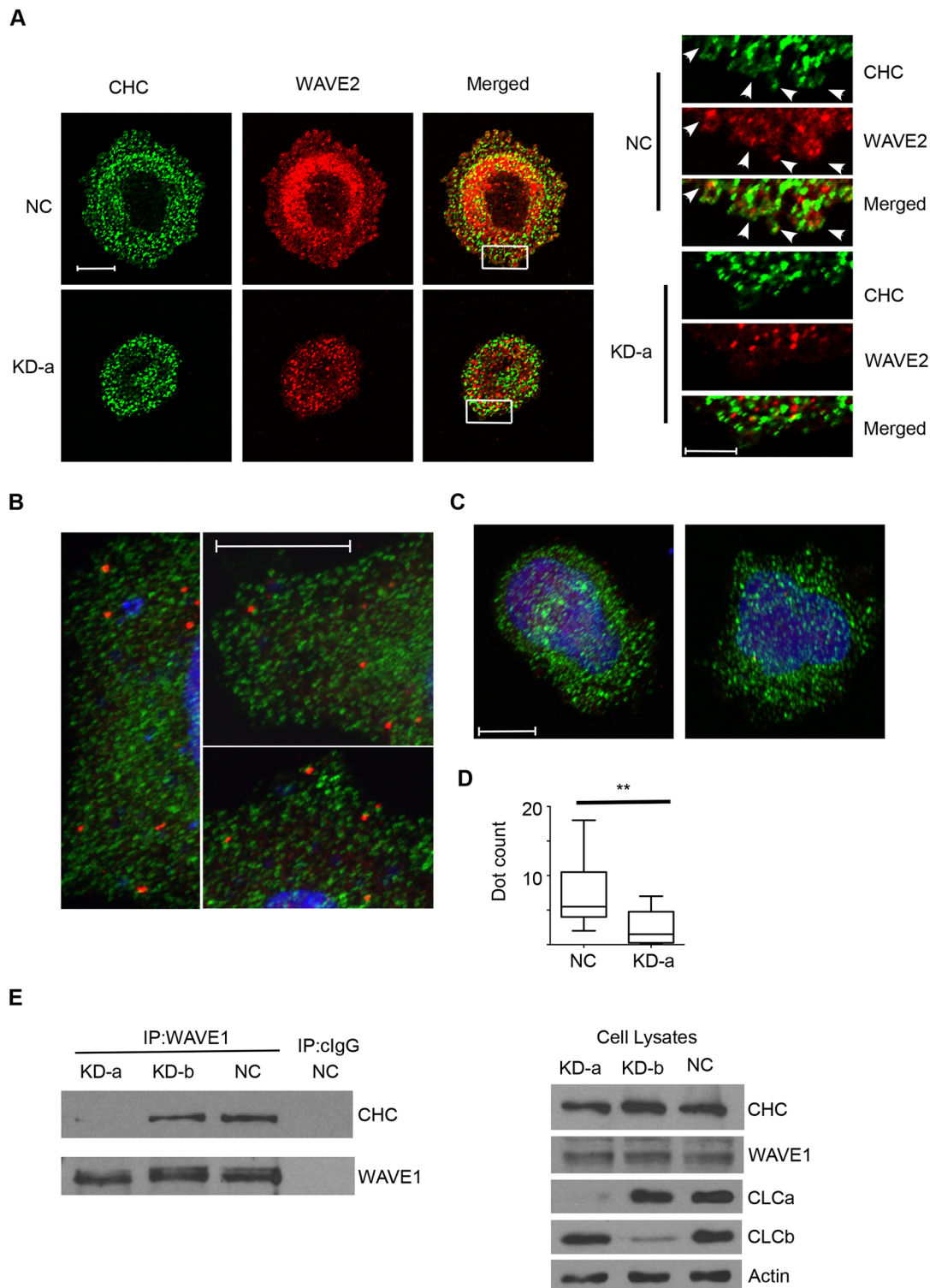


**Fig. 3. Downregulation of CLCa expression alters interaction of clathrin with WAVE during spreading.** (A) siRNA-transfected cells were plated on collagen IV for 1 h, fixed and stained with CHC (ab21679) and WAVE2 antibodies. Deconvoluted confocal image planes at the adherent surface are shown with boxed areas magnified on the right to highlight regions of proximity (NC) or separation (KD-a) of clathrin and WAVE2. Object-based image segmentation analysis (Rizk et al., 2014) of whole-cell z-stacks revealed a significant decrease in Pearson coefficients of colocalization in KD-a compared to NC cells [ $0.564 \pm 0.047$  and  $0.704 \pm 0.029$  (mean  $\pm$  s.d.), respectively,  $P < 0.0005$ ]. Scale bar: 10  $\mu$ m. (B,C) Control (B) and CLCa-depleted cells (C) were plated on collagen IV as above and subjected to an *in situ* proximity ligation assay (PLA) with anti-CHC (green) and -WAVE2 antibodies, as well as DAPI staining of nuclei (blue). Maximum intensity projections of confocal slices in NC cells (three representative fields shown) exhibit PLA-positive loci (red dots). (C) PLA results in KD-a cells (two representative fields). The experiment was performed three times. Scale bars: 10  $\mu$ m. (D) Number of PLA dots per cell was analyzed by *t*-test. The box represents the 25–75th percentiles, the whiskers show the range, and the median is indicated.  $**P < 0.005$ . (E) HeLa cells were lysed 48 h after siRNA transfection and subjected to an immunoprecipitation assay with anti-WAVE1 or control (clgG) antibodies. The western blot on the right represents 2% of input. The data represent one of three separate experiments.

proximal-distal leg vertex, while CLC binding extends along its proximal leg, at ~18 nm in length (Näthke et al., 1992). Given the extended conformation of CLCs and the antibody size, even a direct CLCa–WAVE interaction might put the reporting antibodies near or beyond the ~40 nm maximal interaction distance of the assay. However, in control cells numerous PLA-positive spots were evident, while their number was greatly reduced or virtually absent in KD-a cells (Fig. 3B–D).

Finally, we used antibodies to full-length WAVE1 to assess interactions in lysates of NC, KD-a cells or HeLa cells depleted of only CLCb (Fig. 3E). We found that CHC was indeed co-immunoprecipitated with WAVE1 from NC cells, again consistent with findings of Gautier and colleagues (Gautier et al., 2011). However, clathrin was strikingly absent from immunoprecipitates of KD-a cells, while depletion of CLCb was without effect on this association. Together, these results provide morphological and biochemical evidence of clathrin–WAVE complex association and its dependence on the presence of CLCa.

### Adhesion-induced activation of Src, FAK and paxillin is inhibited in CLCa-depleted cells

Integrin–ECM engagement and subsequent recruitment and activation of signaling and scaffolding proteins drives the initial phase of isotropic spreading following cell attachment to a substrate (Huvener and Danen, 2009; Lawson and Burridge, 2014). Among the proteins recruited to nascent FAs are FAK (also known as PTK2), Src and paxillin, each of which is activated by intra- or inter-molecular tyrosine phosphorylation events (reviewed in Harburger and Calderwood, 2009). Accordingly, we next turned to look at these signaling events that occur upstream of Rac activation. We first asked whether HeLa cells that were depleted of CLCa show defects in phosphorylation of these signaling molecules after plating (Fig. 4A). For NC cells in suspension, the levels of phosphorylated Src(Y416) was low while phosphorylated FAK(Y397) and paxillin(Y118) were virtually undetectable, as expected given their adhesion-dependent activation (Connelly et al., 2010; Guan and Shalloway, 1992). The levels of phosphorylation for all these proteins increased on plating, in each case rising to maximal levels at 60 min and declining slightly thereafter (Fig. 4A,B). In contrast, in KD-a cells the increases of phosphorylated forms of all of these proteins were substantially reduced ( $\geq 50\%$ ), with Src phosphorylation most affected and inhibited by ~65–75%.

Initial FAK activation on Y397 is known to induce additional Src-mediated phosphorylation of sites that contribute to further scaffold protein recruitment (Calalb et al., 1995). Consistent with this, phosphorylation of FAK(Y576) and FAK(Y925) sites were observed following plating in NC cells. Again, phosphorylation of these sites was inhibited in KD-a cells compared to controls (Fig. 4C). Similar inhibition of integrin-mediated activation of these proteins also occurred in H1299 cells depleted of CLCa. This included inhibition of tyrosine phosphorylation of Src and paxillin, and more modestly of FAK, in KD-a cells compared to controls (Fig. S4A), as well as the Src-mediated phosphorylation of the additional sites in FAK (Fig. S4B). Importantly, depletion of CLCb was without effect on Src phosphorylation or on phosphorylation of the primary FAK or Src-mediated FAK sites in H1299 (Fig. S4B) or HeLa cells (data not shown).

H1299 cells spread and move more rapidly than HeLa cells. Interestingly protein phosphorylation was also inhibited at earlier time points in H1299 than in HeLa cells; within 10–20 min of plating, Src and paxillin were significantly diminished (~50–65%) compared to controls (Fig. S4A). Notably, in both H1299 and HeLa

cells, these phosphorylation differences precede the inhibition of spreading (compare Fig. 1). Taken together, these results indicate that activation of these key proteins for FA formation and stabilization are substantially blunted in cells depleted of CLCa but not CLCb, contributing to a reduced ability to effectively spread after plating.

### Recruitment of adhesion and signaling molecules to the spreading surface and FA maturation are aberrant in CLCa-depleted cells

Integrin-activated signaling and scaffolding molecules are recruited to nascent focal complexes, some of which mature to form FAs, which are required to support cell spreading and protrusion formation (Wolfenson et al., 2013; Wozniak et al., 2004). The localization of two key FA proteins near the adherent surface, activated (phosphorylated) FAK (pFAK) and paxillin, was monitored by immunofluorescence microscopy during the 2 h after plating in control and KD-a HeLa cells (Fig. 5A). In both control and KD-a cells at 15 min after plating, both proteins were initially distributed in punctate patterns throughout the cell field or partially localized to peripheral loci. Within 30 min in NC cells, the majority of the proteins near the adherent surface had been substantially recruited to nascent focal adhesions and focal complexes at the cell periphery. By 60–120 min after plating, the initially radially symmetric shape of control cells had developed into an asymmetric profile with protrusions anchored by mature FAs decorated by both proteins, as expected during normal cell spreading (Xiong et al., 2010). In contrast, CLCa-depleted cells maintained a more circular, generally symmetric and less spread shape throughout the entire time period and failed to develop well-formed mature FAs, as also discernible in lower magnification phase-contrast images of cell populations (Fig. S1).

Confocal *x-y* and *y-z* sections of pFAK- and paxillin-stained control cells at 60 min after plating (Fig. 5B) showed that both proteins were colocalized in well-defined FAs at the adherent surface of NC cells, as expected (Parsons et al., 2000; Turner, 2000). Furthermore, almost all pFAK had been recruited to the adherent surface; while this was also true for paxillin, some of the latter could also be detected internally above the adherent surface (marked by a thin orange line in *y-z* projections in Fig. 5B). In contrast, in KD-a cells, larger proportions of both proteins than in controls had failed to be recruited to the adherent surface and were present on the upper plasma membrane surface and intracellularly as punctate signal, likely on vesicular structures. Furthermore, structures marked by colocalized paxillin and pFAK on the adherent surface revealed assembly of fewer and more-poorly defined FAs. Quantification of the number of mature FAs (defined as those  $\geq 2 \mu\text{m}$  in length and radially oriented) during spreading supported this inference, revealing an inhibition in FA number in KD-a cells of ~50% at 30 min after plating (Fig. 5C). To examine this more closely, we used total internal reflection fluorescence (TIRF) microscopy images of pFAK-stained cells plated for 60 min (Fig. 5D). While mature FAs predominated in control cells, the vast majority of pFAK (and paxillin, data not shown) staining in KD-a cells was present in circumferential segments, characteristic of immature focal adhesions or complexes. Interestingly, the average length of individual pFAK segments (either radial or circumferential) was essentially identical in both NC and KD-a cells. However, in KD-a cells the number of mature FAs per cell was reduced by more than 65%, while the total length per cell of circumferential structures was more than 6-fold higher than in control cells (Table S1). Taken together, these results indicate that, in cells depleted of CLCa, maturation of adhesion complexes failed to progress beyond

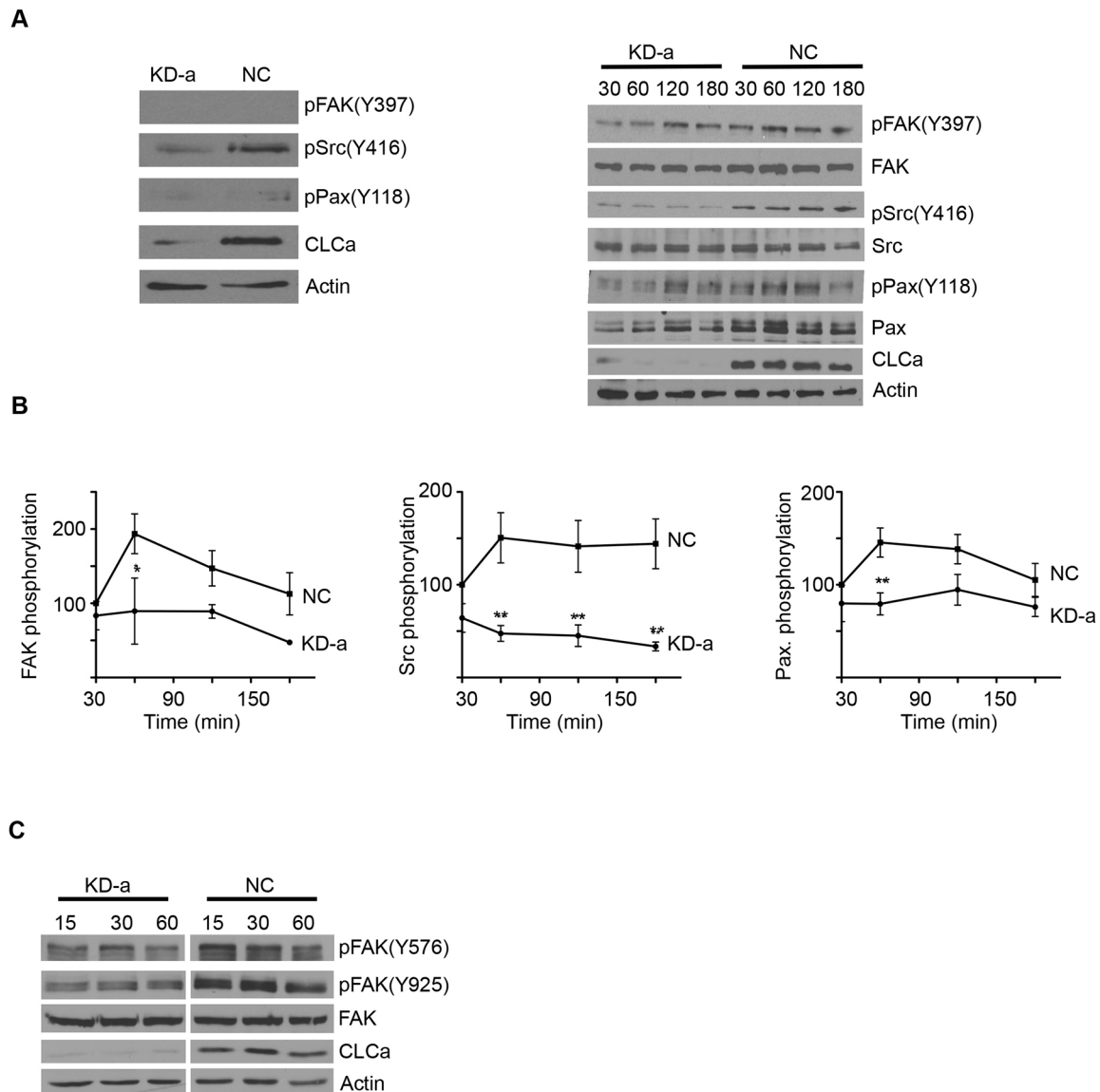


**Fig. 4. CLCa depletion significantly inhibits spreading-induced signaling.** (A) siRNA-transfected cells held in suspension for 1 h (left panel) or plated on collagen IV-coated dishes for the indicated times (minutes, right panel) were lysed and subjected to western blotting with anti-active FAK [pFAK(Y397)], active Src [pSrc(Y416)] and anti-phosphorylated paxillin [pPax(Y118)] antibodies. (B) Protein phosphorylation in control cells at 30 min after plating was set as 100%. The results represent a summary from five to seven experiments. \* $P < 0.05$ ; \*\* $P < 0.01$ . (C) Lysates from plated cells treated as in A were analyzed by western blotting with antibodies against Src-dependent FAK phosphorylation sites (Y576 and Y925). The blots shown represent one of three independent experiments.

recruitment and initial organization of the proteins on the surface, which then grow to a uniform length.

It is known that maturation of FAs requires turnover of the structures and their components (Ezratty et al., 2009; Nader et al., 2016) in a microtubule-dependent manner. Accordingly, we used nocodazole synchronization (Ezratty et al., 2005) to ask whether depletion of CLCa affects FA disassembly or reformation. After incubation with nocodazole for 4 h to block microtubule-dependent FA disassembly, nocodazole was washed out and the cells were followed for the next 60 min. In both control and KD-a cells, washout revealed loss of mature FAs during the initial 30 min, as previously reported (Ezratty et al., 2005). However, while robust FA regrowth during the following 30 min was evident in control cells, it was noticeably diminished in KD-a cells (Fig. 6A). Again, the NC cells revealed formation of mature, radially elongated FAs, while predominantly circumferential segments were observed in KD-a cells (Fig. 6A, insets). Quantification of mature FAs (Fig. 6B)

confirmed these impressions, with comparable levels of FA disappearance observed initially on nocodazole washout in both cell samples, but with a 40–50% decrease in reformation of mature FAs in KD-a cells from 30–60 min after nocodazole removal.

To examine the effect of CLCa depletion on the morphological relationship between clathrin and FAs under spreading conditions, we immunostained for pFAK and clathrin in NC and KD-a cells at 60 min after plating (Fig. 7). In control cells, FAs marked by pFAK staining were often adjacent to or overlapped with small clathrin puncta in the cell periphery (Fig. 7, upper panel, arrowheads; and see below), consistent with the role of clathrin in FA turnover as has previously been suggested (Chao and Kunz, 2009; Ezratty et al., 2009; Gautier et al., 2011). In contrast, in KD-a cells the clathrin and pFAK signals were more separated. Here, clathrin structures terminated noticeably interior to surrounding pFAK signal (Fig. 7, magnified images), the latter often present in circumferential segments highlighted by TIRF microscopy



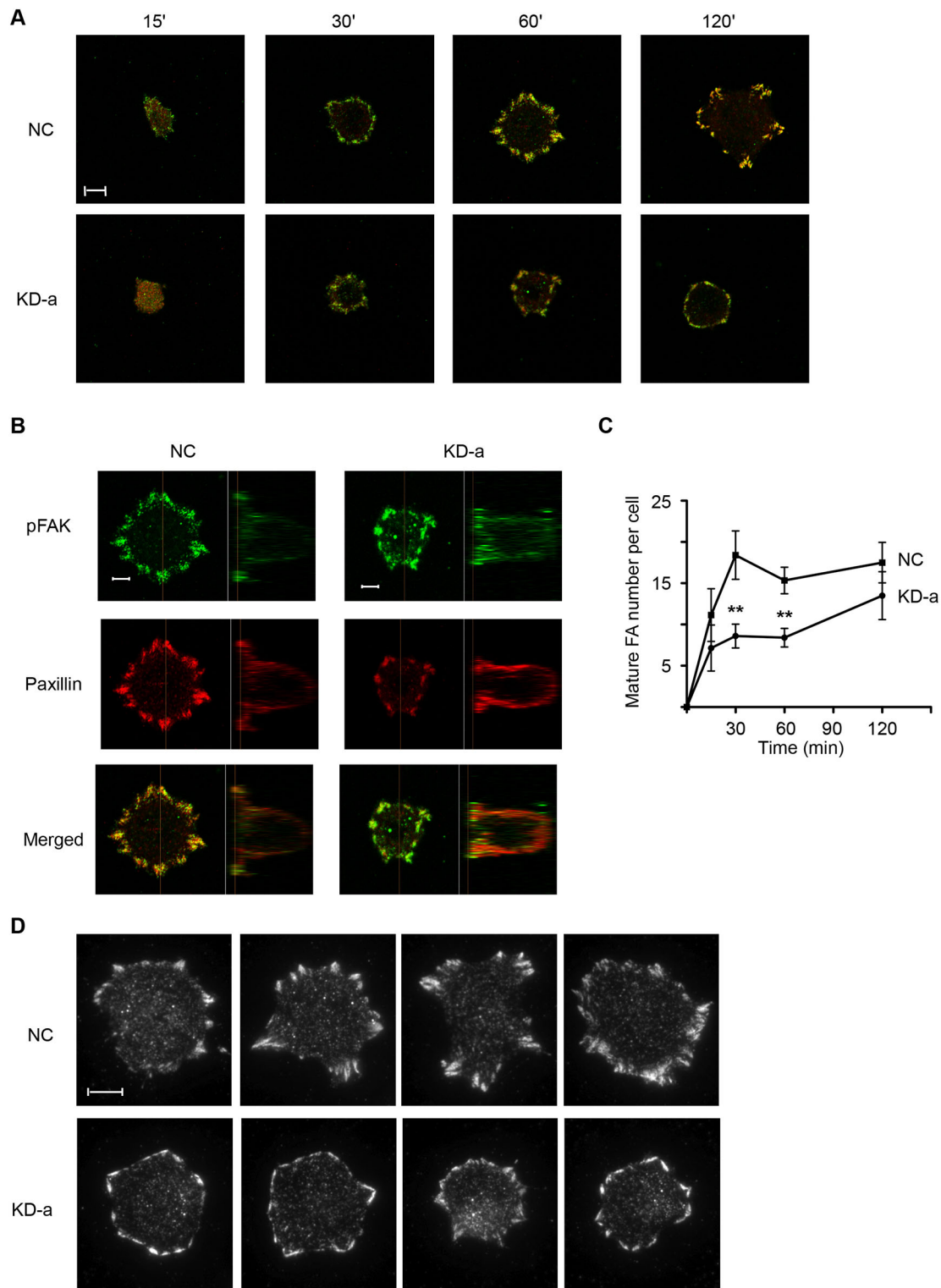


**Fig. 5. CLCa knockdown inhibits recruitment of FAK and paxillin to, and maturation of, FAs.** (A) siRNA-transfected HeLa cells were plated on collagen IV-treated glass coverslips for 15–120 min, and fixed and stained with anti-pFAK(Y397) (pFAK, green) and -paxillin (red) antibodies. Single confocal sections near the adherent surface were obtained as described in the Materials and Methods. Scale bar: 10  $\mu$ m. (B) Representative x-y image planes near the adherent surface, with y-z projections on the right, are shown for cells processed as in A. Scale bars: 5  $\mu$ m. (C) Quantification of the number of mature (longer than 2  $\mu$ m) FAs per cell in siRNA-transfected HeLa cells plated on collagen IV coverslips for 15–120 min. The graph represents a summary of three experiments. \*\* $P < 0.005$ . (D) Representative TIRF microscopy images of phosphorylated FAK (pY397) in siRNA-transfected cells processed as in A. Scale bar: 5  $\mu$ m.

(Fig. 5). Furthermore, the finer clathrin puncta noted above in NC cells were much less apparent. Together, these results show that, in CLCa-depleted cells, clathrin coat structures are present in an

intermediary region, that is noticeably separate from both the more centripetal WAVE labeling (Fig. 4A) and the more peripheral FAs.



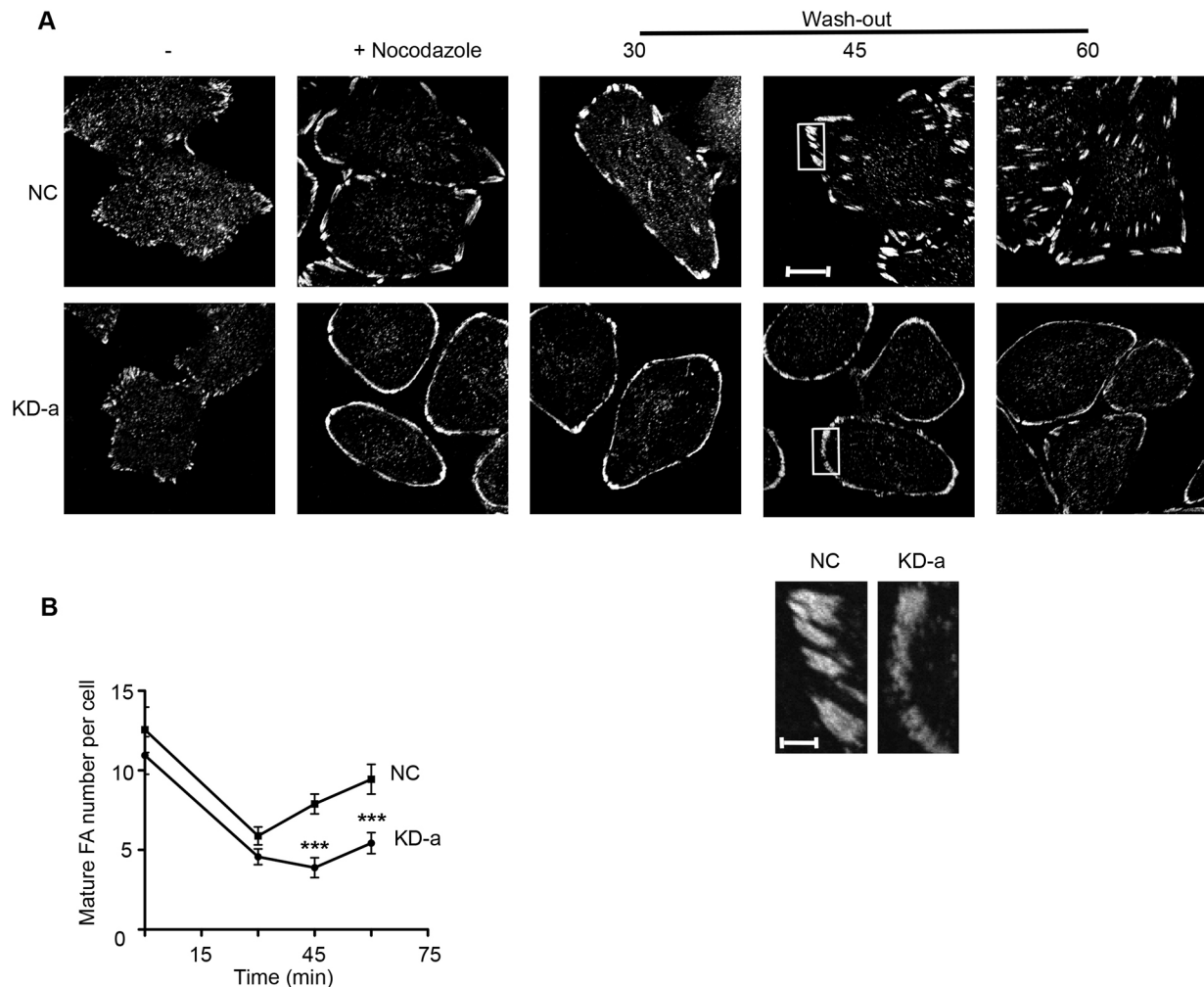


**Fig. 6. CLCa depletion does not affect FA disassembly but inhibits FA recovery after nocodazole washout.** (A) HeLa cells were treated with nocodazole to block FA disassembly, followed by washout for 30–60 min. Cells were fixed and stained with anti-paxillin antibody. Scale bar: 10  $\mu$ m. The lower panels represent magnifications of the boxed areas at 45 min. Scale bar: 2  $\mu$ m. (B) Quantification of the number of mature FAs per cell in siRNA-transfected HeLa cells after nocodazole treatment (time 0) and washout for 30–60 min. \*\*\* $P$ <0.0005. The experiment was performed four times.

### CHC and CLCs in protrusions of spreading cells

To further evaluate the nature of clathrin structures in the periphery of spreading cells, we immunostained NC cells with antibodies to CHC and CLCb: unfortunately, specific antibodies to CLCa for native immunostaining were not available. Confocal microscopy images of the bottom surface (Fig. 8A) showed that most clathrin-coated structures in interior regions of the spreading cell were labeled by both CHC and CLCb, as expected. We note that there appeared to be variations in the CLCb:CHC ratios throughout the cell, with higher levels in the TGN (data not shown), but this was not pursued further here. However, TIRF microscopy (Fig. 8B) revealed that, in protrusions, while the CLCb signal was present in some structures, most puncta (short arrowheads) and nearby areas of more diffuse CHC staining (long arrowheads) had distinctly low or absent CLCb signal. Close inspection of confocal images also suggested lower levels of CLCb in these structures (Fig. 8A, inset).

We used a well-characterized monoclonal antibody to CHC (X22) to confirm that visualization of the CHC signal in the cell protrusions was not antibody dependent. Confocal and TIRF imaging (Fig. S5A) of CHC showed similar results to those found with the rabbit antibody, with smaller, finer puncta and nearby regions of more continuous CHC staining in cell protrusions that were prominent in

TIRF microscopy images (arrowheads), suggesting that both were on the adherent surface. When cells were allowed to grow for 24 h, the proportion of this staining in relation to the canonical coated pit signal decreased markedly, with both anti-CHC antibodies, as seen in both confocal and TIRF microscopy images (Fig. S5B). Finally, coated pits in the plasma membrane resist mild detergent extraction in many cells, likely through close association with the cortical actin meshwork (Beck and Nelson, 1996; Collins et al., 2011; Gaidarov et al., 1999; Morone et al., 2006). When cells plated for 60 min were briefly permeabilized before fixation, coated pits persisted but a substantial decrease in the background CHC staining was evident, and CHC–CLCb colocalization increased dramatically (Fig. S5C). Taken together, these results suggest that, in spreading cells, CLCb-lacking clathrin structures represent a fraction of coat structures that are distinct from canonical coated pits.

The individual clathrin coat structures of pits, vesicles and tubule buds are smaller than the diffraction limit of conventional light microscopy, while clusters or plaques can be considerably larger. Accordingly, we infer that the dimmer, but distinct, puncta in spreading regions of HeLa cells contain fewer triskelia and are perhaps assembling coat structures, in contrast to the brighter coated pits located across the bottom plasma membrane of the cell.

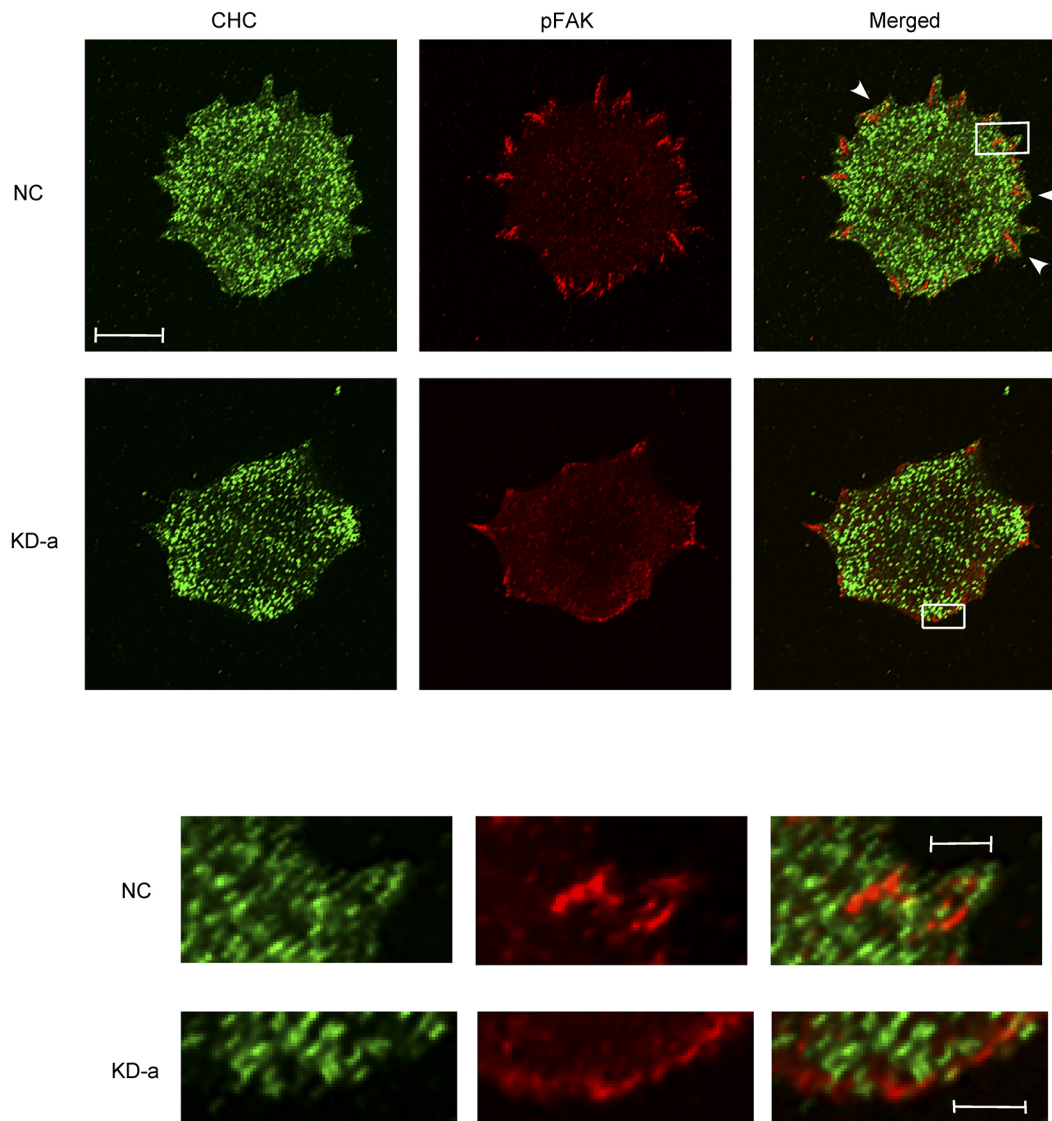


**Fig. 7. CLCa knockdown decreases the colocalization of clathrin and pFAK in the lamellipodial region of HeLa cells.** siRNA-transfected cells were plated on collagen IV for 1 h, fixed and co-stained anti-pFAK(Y397) (pFAK) and CHC (ab21679) antibodies. Representative deconvolved confocal images are shown, with arrowheads in NC indicating areas containing pFAK staining in close proximity to fine clathrin puncta. Enlargements of the boxed areas in NC and KD-a cells are shown underneath. The experiment was performed three times. Scale bars: 10  $\mu$ m; 2  $\mu$ m in insets.

Furthermore, we speculate that the nearby, more continuous CHC staining may be incompletely assembled lattice fragments that are spread over a broader surface. Importantly, both of these forms of clathrin are relatively deficient in CLCb, and are prominent in protrusions of spreading cells. These regions are also sites of punctate cortactin and F-actin staining (Fig. 8C), consistent with the small lamellipodia characteristic of HeLa cells (Gautier et al., 2011; Majeed et al., 2014; Yang et al., 2007), as well as pFAK localization (Fig. 7).

Finally, in the absence of appropriate CLCa antibodies, we used an exogenous expression approach to directly ask whether CLCa could be identified in the protrusive regions of spreading cells. KD-a cells expressing low levels of epitope-tagged CLCa-R, in amounts comparable to endogenous CLCb, were imaged by TIRF microscopy (Fig. 8E). As expected, co-staining of clathrin coat structures containing both CLCa-R and CLCb was evident in structures located towards the cell interior. However, in protrusions, the characteristic CLCb-deficient CHC puncta (arrowheads) and larger more continuous structures (arrows) lacking CLCb were seen

(Fig. 8E). Taken together, these observations provide direct evidence of the presence of CLCa and comparative absence of CLCb in clathrin structures in the protrusive regions of spreading cells.

## DISCUSSION

Spreading in newly attached cells is driven by actin reorganization and association with myosin to generate force against membrane tension, thereby extending lamellipodia outward (Pollard and Borisy, 2003). This initial radial enlargement and subsequent anisotropic extension of a small number of protrusions, resulting in an asymmetric profile, have been well characterized as the first and second phases in cell spreading (Fardin et al., 2010; Rangamani et al., 2011). In cells depleted of CLCa, some initial spreading, comparable in extent to that in NC cells, was observed. However, both completion of the initial isotropic spreading phase and subsequent development of protrusions and anisotropic spreading were greatly inhibited in CLCa-depleted, but not CLCb-depleted, cells. Accordingly, rather than becoming asymmetric and

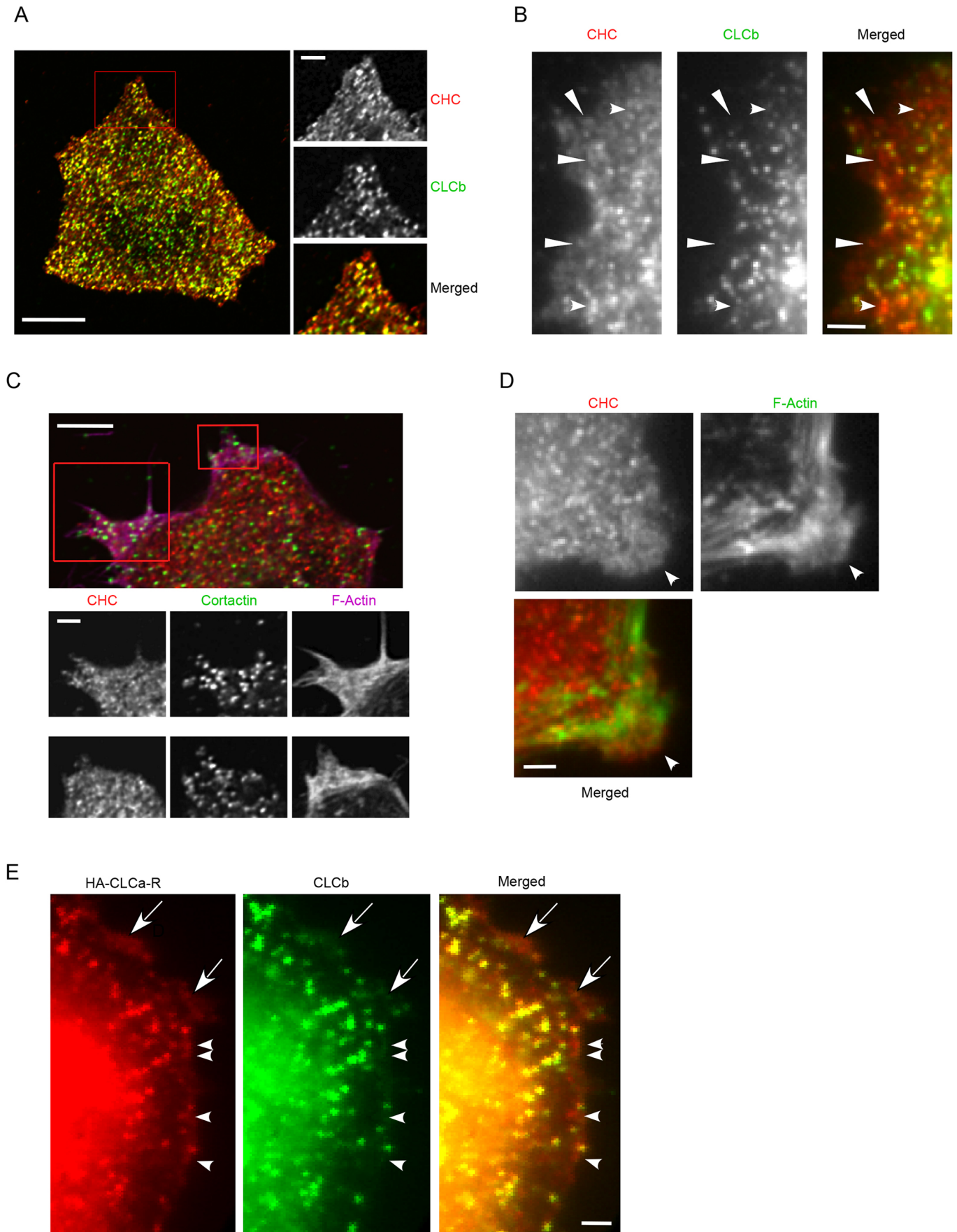


Fig. 8. See next page for legend.



**Fig. 8. CLCb-deficient clathrin structures in protrusions of spreading cells.** HeLa cells were plated for 60 min, then fixed and processed as indicated. (A,B) Cells immunostained for CHC (ab21679) and CLCb and imaged by confocal microscopy at the adherent surface (A) or by TIRF microscopy (B). Peripheral CHC structures comparatively deficient in CLCb signal are detectable in the confocal image (insets), and are more apparent by TIRF imaging (B) as multiple CHC-containing puncta (short arrowheads) and regions with less punctate staining (long arrowheads). Scale bar: 10  $\mu$ m (main image in A); 2  $\mu$ m (magnified images in A and B). Results are representative of five experiments. (C) Both F-actin (stained with SiR-actin) and cortactin are present in protrusions containing small CHC puncta, as imaged by confocal microscopy. Scale bars: 5  $\mu$ m (main image); 2  $\mu$ m (magnifications). (D) TIRF microscopy reveals F-actin (Alexa Fluor 546–phalloidin) and CHC staining in a protrusion (arrowhead). Scale bar: 2  $\mu$ m. (E) Spreading region in the periphery of a KD-a cell expressing HA–CLCa-R and immunostained for HA and CLCb. TIRF microscopy reveals diffuse (arrows) and punctate structures (arrowheads) containing CLCa with low or undetectable levels of CLCb. Scale bar: 2  $\mu$ m. Representative of five independent experiments.

progressively flattened, the former maintained a characteristic tall profile reminiscent of a ‘top hat’ shape, and exhibited reduced rates of migration as measured in wound closure and motility assays.

CLCa depletion exerts these changes as a result of several interrelated effects on integrin-mediated activation, actin rearrangements and FA maturation. First, inhibition of sustained integrin-mediated activation of the key signaling and scaffolding proteins FAK, paxillin and Src were a prominent effect in cells depleted of CLCa, but not of CLCb. Integrin-mediated signaling was adequate to support cell attachment and initial spreading, as well as formation of nascent adhesions and focal complexes, but may not be sufficient to support growth beyond this initial phase. The molecular defects resulting from loss of CLCa that block full integrin-mediated signaling remain to be elucidated, but may include loss of physical proximity with key intermediates, such as FAK reported here, and more generally with effector scaffold proteins including Src, talin, kindlin and paxillin and others (Theodosiou et al., 2016; Zhang et al., 2008). A related casualty of depletion of CLCa was a failure to fully organize F-actin. Rather, in KD-a cells F-actin was predominantly present as short, randomly organized filaments or bundles. Our work suggests this results, at least in part, from loss of CLCa-dependent biochemical association of clathrin with the nucleation-promoting factor WAVE, resulting in separation of the two complexes as demonstrated *in situ*. The functional importance of the clathrin–WAVE association in lamellipodial formation (Gautier et al., 2011; Ramirez-Santiago et al., 2016) is complemented by the observations that depletion of N-WASP disrupts interactions of F-actin with both clathrin-coated pits and with flat plaque structures in the cell periphery (Galovic et al., 2011; Leyton-Puig et al., 2017).

A key defect in cells depleted of CLCa is a block in maturation of FAs. Assembly of pFAK- and paxillin-containing nascent adhesions and focal complexes was observed, circumferentially decorating substantial portions of the plasma membrane. However, this normally transient organization largely failed to mature to a radially elongated FA. Interestingly, the average length of pFAK-stained segments, either circumferential or radial, that we observe in NC and KD-a cells are indistinguishable (Table S1), suggesting a mechanistic limitation to their growth. Accordingly, although the number of mature FAs was greatly reduced in KD-a cells, far more membrane was restricted to focal complexes in these cells. Of particular relevance in this context is the observation of Horwitz and colleagues (Choi et al., 2008) showing that depletion of  $\alpha$ -actinin or the actin-bundling activity of myosin II resulted in similar (though less extensive) accumulation of circumferential focal complexes and inhibition of FA maturation, which was attributed to loss of  $\alpha$ -actinin and actin-defined tracks

supporting radial elongation of maturing FAs. Together, our results suggest the CLCa-dependent reduction in integrin-mediated activation of Src and Rac which are key to recruitment of paxillin and WAVE to FAs (Chen et al., 2017a; Lebensohn and Kirschner, 2009; Palamidessi et al., 2008), fail to provide the branched F-actin formation required for tension production and FA maturation. The molecular defects resulting from loss of CLCa that block full integrin-mediated signaling remain to be elucidated, but may include loss of physical proximity with key intermediates, such as FAK, and other effector scaffold proteins, or other alterations in clathrin-mediated membrane trafficking.

The fine CHC staining (small, defined puncta and nearby areas of more diffuse signal) that we identify here in protrusive regions of spreading HeLa cells in proximity to WAVE2 and pFAK (Figs 3, 7 and 8) is detectable but less evident after spreading (e.g. fig. S5B and fig. 1A,D in Leyton-Puig et al., 2017). That CLCb is reduced or absent in these structures while exogenous CLCa colocalizes with them in rescued KD-a cells (Fig. 8), provides important support for a specific role for CLCa in spreading. These areas appear to lack the adaptor protein 2 (AP-2) complex but may have other adaptors of endosomal compartments (Calabia-Linares et al., 2011; Gautier et al., 2011; Ramirez-Santiago et al., 2016). It is tempting to speculate that they comprise newly formed clathrin lattices whose CLCa components are key for efficient recruitment of nucleation-promoting factor and actin, and ensuing branched actin formation. Subsequently, CLCb-containing triskelia might be added as these structures mature and FA formation progresses.

When not attached to clathrin triskelia, the two CLCs are unstructured polypeptides that tend to become rapidly degraded *in situ* (Brodsky, 1985; Hinrichsen et al., 2003; Poupon et al., 2008). This raises the possibility that loss of function upon depletion of CHC, as often performed in tests for clathrin involvement in cellular processes, may actually reflect loss of a specific CLC function. The light chains share ~60% sequence identity overall in Chordata (Jackson et al., 1987), including a highly conserved 22-residue sequence that links clathrin to actin through Hip1-binding proteins (Engqvist-Goldstein et al., 1999). While this sequence is critical for actin organization around plasma membrane coated pits, as well as actin-dependent clathrin-mediated internalization of pathogens and other large structures (Brodsky, 2012; Humphries and Way, 2013), the unique effects reported here indicate that CLCa-specific interactions also exist. Determining whether these may provide novel targets for blocking oncogenic aspects of integrin-mediated signaling or the movement and reattachment of malignant cells critical for metastasis are important new questions raised by this work.

## MATERIALS AND METHODS

### Cell lines and transfections

All cell lines were obtained from the American Type Culture Collection (ATCC). HEK293 and HeLa cell lines were grown in Dulbecco’s modified Eagle’s medium (DMEM) supplemented with 10% fetal bovine serum (FBS) and antibiotics. H1299 cells were propagated in RPMI1640 supplemented with 10% FBS and antibiotics. Cell transfections were carried out using Hiperfect (Qiagen 301705) for siRNA, and Lipofectamine 3000 (Invitrogen L3000-008) for DNA according to the manufacturers’ instructions. For siRNA transfections, the cells were plated in the growth medium in the presence of siRNA/Hiperfect complexes and grown for 48–72 h. siRNA-resistant DNA was added 24 h after the start of siRNA transfection and the cells were analyzed after 24–48 h.

### siRNA and primers

For CLC knockdown, the following siRNAs were used: CLCa siRNAs from Dharmacon (5’-AGACAGUUAUGCAGCUAAU-3’) (Huang et al., 2004)

and Qiagen (SI04220153, 5'-GGAAAGUAAUGGUCCAACATT-3'), CLCb siRNAs from Dharmacon (5'-GGAACGACGCCAGAGUGAU-U-3') (Huang et al., 2004) and from Qiagen (SI00348733, 5'-CAGCGC-CAGAGTGAACAAGTA-3'). Negative control siRNA was purchased from Qiagen (1027310, 5'-UUCUCCGAACGUGUCACGU-3'). siRNA-resistant (against Dharmacon's CLCa siRNA) DNA was obtained by mutagenesis of a mouse (m)CLCa DNA (Zhao et al., 2007) using QuikChange II XL kit (Agilent Technologies, 200521-5) and primers: 5'-ACTTCTGAAATGGCTGCGTAAGAATCTGTTGGACCATGCTCTCC-3' and 5'-GGAGAGCAATGGTCCAACAGATTCTTACGCGACCCATTTT-AGAAGT-3'. Both wild-type and mutated mCLCa DNAs were cloned into Flag-HA-pcDNA3.1 vector from Addgene (52535, Horn et al., 2014).

### Cell spreading assay

At 48 h post-transfection, cells were trypsinized, briefly centrifuged in growth medium (14,000 *g* for 5 min), resuspended in FBS-free medium and incubated for 1 h at 37°C. After incubation, the cells were plated on collagen IV (Corning 354233)-treated glass coverslips for different time points and fixed with 3.7% formaldehyde in PBS. Immunofluorescence staining was performed as published previously (Tsygankova et al., 2010). Widefield images were taken on a Zeiss Axiovert 200M microscope supplied with 20×/0.8 NA objective and Evolve 512M camera (Photometrics). Cell area analysis was undertaken using MetaMorph software (Universal Imaging). Data from 5–7 plating experiments were summarized together, and normalized to the mean area of control cells plated for 30 min. For live-cell phase-contrast imaging, siRNA-transfected cells were serum starved in suspension for 1 h, then plated on 35 mm glass-bottom dishes (Mattek) treated with collagen IV. Cell adhesion was monitored by the IncuCyte S3 Live Cell Analysis System (Essen Bioscience) with phase-contrast images of 12 fields per dish taken at the indicated time points.

### Immunofluorescence analysis

Confocal imaging was performed on Nikon A1R or C2 inverted confocal microscopes, using a 60×/1.4 NA objective. Z-stack, 3D automatic deconvolution and FA analysis were performed using NIS Elements software (Nikon). Z-stack imaging was performed with 0.35–0.7  $\mu\text{m}$  z-steps and 3–4× zooming. TIRF microscopy was performed on fixed samples mounted in PBS on a Nikon TiE inverted microscope with TIRF E motorized illuminator using a 100×/1.49 NA objective, Andor 488/561 nm lasers, DualView2 beamsplitter (Photometrics) and captured with an Andor Ion X3 EM-CCD camera controlled by MetaMorph software (Universal Imaging). Evaluation of clathrin–WAVE2 colocalization was performed with an object-based image segmentation method using the Fiji plugin SQUASSH (Rizk et al., 2014) operating on complete native confocal cell stacks. For immunofluorescence staining, antibodies against the following proteins were used: phosphorylated FAK(Y397) (1:300, 44-624G), CHC (1:500, X22, MA1-065), paxillin (1:300, 612405) from BD Pharmingen, CHC (1:500, ab21679), paxillin (1:300, ab32084) from Abcam, phosphorylated FAK(Y397) (1:200, MAB4528) from RD Systems, WAVE2 (1:200, sc-373889 or 1:200, #3659) from Santa Cruz Biotechnology and Cell Signaling, respectively, and cortactin (1:200, #3503) from Cell Signaling. F-actin staining was performed with Alexa Fluor 546-labeled phalloidin (Molecular Probes, A22283) or SiR-actin (Cytoskeleton, CY-SC001). Alexa Fluor-labeled secondary antibodies were from Life Technologies (Invitrogen).

### Nocodazole treatment

24 h after siRNA transfection, cells were plated on glass coverslips and grown for 24 h. To dissociate microtubules, cells were treated with 10  $\mu\text{M}$  nocodazole (Tocris 1228) in serum-free medium for 2 h (Ezraty 2005, #455). The inhibitor was washed out, and cells were incubated in serum-free medium for 30–60 min followed by fixation and staining with anti-paxillin antibody. FAs were analyzed by confocal microscopy as described above. FAs longer than 2.0  $\mu\text{m}$  were denoted as mature (Kim and Wirtz, 2013).

### Cell adhesion, wound and time-lapse experiments

To determine plating efficiency, siRNA-transfected cells were seeded for 10 min or 2 h on collagen IV-coated 24-well plates in serum-free medium,

fixed and stained with 1% Crystal Violet. After washing and lysis in 1% sodium deoxycholate, the absorbance was read at 590 nm (Tsygankova et al., 2010). For wound assay, confluent cells were starved for 24 h, scratched (three or four wounds per siRNA) and allowed to recover in growth medium for 20 h. Widefield images were taken after the wounding and recovery, and analyzed with MetaMorph software. For the motility assay, time-lapse analysis was performed on a widefield Zeiss microscope with a 10×/0.3 NA objective. Cells were plated on an eight-well chamber slide, and images were taken every 10 min for 18 h. Single-cell tracks were analyzed with ImageJ software as previously described (Tsygankova et al., 2013), using the Chemotaxis and Migration Tool plugins.

### Flow cytometry

After 48 h transfection, cells were harvested and incubated with antibodies against inactive [mAb 13 (1:300, 552828, BD), 4B4 (1:200, 6603113, Beckman Coulter)] or active [12G10 (1:200, MAB2247, Millipore), 9EG7 (1:300, 553715, BD)]  $\beta$ 1-integrin for 1 h on ice followed by staining with Alexa Fluor-labeled secondary antibodies (1 h, 4°C). All antibodies were diluted in cold FACS buffer (PBS with 0.1% BSA). Fluorescence intensity was analyzed on a FACSCalibur system (Becton Dickinson) by using FlowJo software.

### Integrin endocytosis and recycling

siRNA-transfected cells were incubated in suspension for 1 h and plated on collagen IV-coated glass coverslips for 1 h. The cells were then incubated with anti- $\beta$ 1-integrin antibody (mAb 13, 0.17 mg/ml in serum-free medium) on ice for 1 h, and were then fixed or transferred to 37°C medium for 10–60 min to stimulate integrin endocytosis (Arjonen et al., 2012). After fixation and permeabilization, the cells were stained with Alexa Fluor 546-conjugated goat anti-rat-IgG (Life Technologies, A11081) antibody and analyzed by confocal fluorescence microscopy. The integrated cell intensity was analyzed with the MetaMorph program using background correction and stacks arithmetic functions. For evaluation of  $\beta$ 1-integrin recycling, cells incubated with mAb 13 as above were warmed for 30 min to allow uptake and were then washed, fixed and reincubated without permeabilization and with additional mAb 13 followed by Alexa Fluor 488-conjugated anti-rat-IgG antibody to label surface  $\beta$ 1-integrin antibody. They were then washed, permeabilized and stained with Alexa Fluor 546-conjugated goat anti-rat-IgG antibody to reveal internal  $\beta$ 1-integrin.

### Rac1 activation assay

The pull-down activation assay was performed using a kit from Cytoskeleton (BK035-5). siRNA-transfected cells were kept in suspension for 1 h as described above, then plated on collagen IV-treated dishes for the indicated times. Cells were lysed and activated Rac1 was retrieved according to the manufacturer's instructions. After western blotting with anti-Rac1 antibody, Rac1-GTP and total Rac1 were analyzed by ImageJ software. After normalization against total protein, Rac1 activation at 15 min in the control cells was set as 100%. The experiment was performed four times.

### Western blotting

After incubation in serum-free medium, cells were plated on collagen IV-coated dishes for the indicated time and lysed with the RIPA buffer (10 mM Tris-HCl pH 7.8, 140 mM NaCl, 1% Triton X-100, 0.1% SDS and 0.5% sodium deoxycholate) supplemented with protease and phosphatase inhibitors (Pierce, A32959). Antibodies against the following proteins were used: CLCa (1:1000, sc-28276), CLCb (1:500, sc-376414), actin (1:1000, sc-1616) from Santa Cruz Biotechnology, FAK (1:2000, 610088) and  $\beta$ 1-integrin (1:1000, 610467) from BD Transduction Labs, phosphorylated FAK(Y397) (1:1000, 44-624G), phosphorylated paxillin(Y118) (1:1000, 44-722G) from Fisher Scientific, Src (1:2000, 2108), phosphorylated Src(Y416) (1:1000, MAB2685, 2101), phosphorylated FAK(Y576) (1:1000, 3281), FAK(Y925) (1:1000, 3284) from Cell Signaling, phosphorylated Src(Y416) (1:1000, MAB2685) from RD Systems, WAVE1/Scar (1:1000, 07-037), Rac1 (1:2000, 05-389) from Millipore. The intensity of protein bands was analyzed by ImageJ software. Protein phosphorylation at 30 min after plating in control cells was set as 100%.



### Immunoprecipitation assay

Cells were lysed in lysis buffer (20 mM Tris-HCl pH 7.8, 100 mM NaCl, 1% Triton X-100 plus protease/phosphatase inhibitors). Cleared cell lysates were incubated with anti-WAVE/Scar antibody (4 µg/ml, Millipore 07-037) for 30 min on ice followed by 2 h incubation with Protein G-agarose on a rotor at 4°C. Immunoprecipitated proteins were subjected to western blot analysis.

### Proximity ligation assay

Cells plated on glass coverslips were stained with the anti-CHC (mouse) and anti-WAVE2 (rabbit, Fisher PA5-60975) antibodies as described above. PLA was performed using the Duolink *in situ* Red PLA kit (#92101) from Sigma, containing specific anti-rabbit-minus and anti-mouse-plus probes. Ligase and polymerase reagents were used according to the manufacturer's recommendations. Nuclei were stained with 0.1 µg/ml DAPI for 5 min at room temperature. After PLA, the cells were additionally stained with Alexa Fluor 488 goat anti-mouse-IgG antibodies for clathrin visualization.

### Statistical analysis

Data were analyzed using Prism program. Graphs shown represent the mean ±s.e.m. obtained from the indicated number of independent experiments. Statistical significance was set at  $P < 0.05$  using an unpaired Student's *t*-test for two group comparisons.

### Acknowledgments

We gratefully acknowledge Drs S. Astrof and L. Languino (Jefferson U.), and T. Svitkina (U. Pennsylvania) for helpful discussions, A. Mazo and S. Petruk (Jefferson U.) for assistance with PLA, C. Rogers and T. Alnemri (Jefferson U.) for assistance with Incucyte imaging, and M. Y. Covarrubias and the Bioimaging Shared Resource of the Sidney Kimmel Cancer Center (NCI 5 P30 CA-56036).

### Competing interests

The authors declare no competing or financial interests.

### Author contributions

Conceptualization: J.H.K., O.M.T.; Methodology: J.H.K., O.M.T.; Software: J.H.K., O.M.T.; Validation: J.H.K., O.M.T.; Formal analysis: J.H.K., O.M.T.; Investigation: J.H.K., O.M.T.; Resources: J.H.K.; Data curation: J.H.K., O.M.T.; Writing - original draft: J.H.K., O.M.T.; Writing - review & editing: J.H.K., O.M.T.; Visualization: J.H.K., O.M.T.; Supervision: J.H.K.; Project administration: J.H.K.; Funding acquisition: J.H.K.

### Funding

This work was supported by the National Institutes of Health (GM-49217 to J.H.K.). Deposited in PMC for release after 12 months.

### Supplementary information

Supplementary information available online at <http://jcs.biologists.org/lookup/doi/10.1242/jcs.224030.supplemental>

### References

- Alanko, J., Mai, A., Jacquemet, G., Schauer, K., Kaukonen, R., Saari, M., Goud, B. and Ivaska, J. (2015). Integrin endosomal signalling suppresses anoikis. *Nat. Cell Biol.* **17**, 1412-1421. doi:10.1038/ncb3250
- Arjonen, A., Alanko, J., Veltel, S. and Ivaska, J. (2012). Distinct recycling of active and inactive beta1 integrins. *Traffic* **13**, 610-625. doi:10.1111/j.1600-0854.2012.01327.x
- Beck, K. A. and Nelson, W. J. (1996). The spectrin-based membrane skeleton as a membrane protein-sorting machine. *Am. J. Physiol.* **270**, C1263-C1270. doi:10.1152/ajpcell.1996.270.5.C1263
- Bierne, H., Miki, H., Innocenti, M., Scita, G., Gertler, F. B., Takenawa, T. and Cossart, P. (2005). WASP-related proteins, Abi1 and Ena/VASP are required for Listeria invasion induced by the Met receptor. *J. Cell Sci.* **118**, 1537-1547. doi:10.1242/jcs.02285
- Brodsky, F. M. (1985). Clathrin structure characterized with monoclonal antibodies. II. Identification of *in vivo* forms of clathrin. *J. Cell Biol.* **101**, 2055-2062.
- Brodsky, F. M. (2012). Diversity of clathrin function: new tricks for an old protein. *Annu. Rev. Cell Dev. Biol.* **28**, 309-336. doi:10.1146/annurev-cellbio-101011-155716
- Brodsky, F. M., Sosa, R. T., Ybe, J. A. and O'Halloran, T. J. (2014). Unconventional functions for clathrin, ESCRTs, and other endocytic regulators in the cytoskeleton, cell cycle, nucleus, and beyond: links to human disease. *Cold Spring Harbor Perspect. Biol.* **6**, a017004. doi:10.1101/cshperspect.a017004
- Byron, A., Humphries, J. D., Askari, J. A., Craig, S. E., Mould, A. P. and Humphries, M. J. (2009). Anti-integrin monoclonal antibodies. *J. Cell Sci.* **122**, 4009-4011. doi:10.1242/jcs.056770
- Calabia-Linares, C., Robles-Valero, J., de la Fuente, H., Perez-Martinez, M., Martin-Cofreces, N., Alfonso-Perez, M., Gutierrez-Vazquez, C., Mittelbrunn, M., Ibiza, S., Urbano-Olmos, F. R. et al. (2011). Endosomal clathrin drives actin accumulation at the immunological synapse. *J. Cell Sci.* **124**, 820-830. doi:10.1242/jcs.078832
- Calalb, M. B., Polte, T. R. and Hanks, S. K. (1995). Tyrosine phosphorylation of focal adhesion kinase at sites in the catalytic domain regulates kinase activity: a role for Src family kinases. *Mol. Cell. Biol.* **15**, 954-963. doi:10.1128/MCB.15.2.954
- Chao, W.-T. and Kunz, J. (2009). Focal adhesion disassembly requires clathrin-dependent endocytosis of integrins. *FEBS Lett.* **583**, 1337-1343. doi:10.1016/j.febslet.2009.03.037
- Chen, C.-Y. and Brodsky, F. M. (2005). Huntingtin-interacting protein 1 (Hip1) and Hip1-related protein (Hip1R) bind the conserved sequence of clathrin light chains and thereby influence clathrin assembly *in vitro* and actin distribution *in vivo*. *J. Biol. Chem.* **280**, 6109-6117. doi:10.1074/jbc.M408454200
- Chen, B., Chou, H. T., Brautigam, C. A., Xing, W., Yang, S., Henry, L., Doolittle, L. K., Walz, T. and Rosen, M. K. (2017a). Rac1 GTPase activates the WAVE regulatory complex through two distinct binding sites. *Elife* **6**, e29795. doi:10.7554/eLife.29795
- Chen, P. H., Bendris, N., Hsiao, Y. J., Reis, C. R., Mettlen, M., Chen, H. Y., Yu, S. L. and Schmid, S. L. (2017b). Crosstalk between CLCb/Dyn1-mediated adaptive clathrin-mediated endocytosis and epidermal growth factor receptor signaling increases metastasis. *Dev. Cell* **40**, 278-288.e5. doi:10.1016/j.devcel.2017.01.007
- Choi, C. K., Vicente-Manzanares, M., Zareno, J., Whitmore, L. A., Mogilner, A. and Horwitz, A. R. (2008). Actin and alpha-actinin orchestrate the assembly and maturation of nascent adhesions in a myosin II motor-independent manner. *Nat. Cell Biol.* **10**, 1039-1050. doi:10.1038/ncb1763
- Collins, A., Warrington, A., Taylor, K. A. and Svitkina, T. (2011). Structural organization of the actin cytoskeleton at sites of clathrin-mediated endocytosis. *Curr. Biol.* **21**, 1167-1175. doi:10.1016/j.cub.2011.05.048
- Connelly, S. F., Isley, B. A., Baker, C. H., Gallick, G. E. and Summy, J. M. (2010). Loss of tyrosine phosphatase-dependent inhibition promotes activation of tyrosine kinase c-Src in detached pancreatic cells. *Mol. Carcinog.* **49**, 1007-1021. doi:10.1002/mc.20684
- D'Souza-Schorey, C., Boettner, B. and Van Aelst, L. (1998). Rac regulates integrin-mediated spreading and increased adhesion of T lymphocytes. *Mol. Cell. Biol.* **18**, 3936-3946. doi:10.1128/MCB.18.7.3936
- Elkhatib, N., Bresteau, E., Baschieri, F., Rioja, A. L., van Niel, G., Vassilopoulos, S. and Montagnac, G. (2017). Tubular clathrin/AP-2 lattices pinch collagen fibers to support 3D cell migration. *Science* **356**. doi:10.1126/science.aal4713
- Engqvist-Goldstein, A. E., Kessels, M. M., Chopra, V. S., Hayden, M. R. and Drubin, D. G. (1999). An actin-binding protein of the Sla2/Huntingtin interacting protein 1 family is a novel component of clathrin-coated pits and vesicles. *J. Cell Biol.* **147**, 1503-1518. doi:10.1083/jcb.147.7.1503
- Engqvist-Goldstein, A. E., Warren, R. A., Kessels, M. M., Keen, J. H., Heuser, J. and Drubin, D. G. (2001). The actin-binding protein Hip1R associates with clathrin during early stages of endocytosis and promotes clathrin assembly *in vitro*. *J. Cell Biol.* **154**, 1209-1223. doi:10.1083/jcb.200106089
- Ezratty, E. J., Partridge, M. A. and Gundersen, G. G. (2005). Microtubule-induced focal adhesion disassembly is mediated by dynamin and focal adhesion kinase. *Nat. Cell Biol.* **7**, 581-590. doi:10.1038/ncb1262
- Ezratty, E. J., Bertaux, C., Marcantonio, E. E. and Gundersen, G. G. (2009). Clathrin mediates integrin endocytosis for focal adhesion disassembly in migrating cells. *J. Cell Biol.* **187**, 733-747. doi:10.1083/jcb.200904054
- Fang, Z., Takizawa, N., Wilson, K. A., Smith, T. C., Delprato, A., Davidson, M. W., Lambright, D. G. and Luna, E. J. (2010). The membrane-associated protein, supervillin, accelerates F-actin-dependent rapid integrin recycling and cell motility. *Traffic* **11**, 782-799. doi:10.1111/j.1600-0854.2010.01062.x
- Fardin, M. A., Rossier, O. M., Rangamani, P., Avigan, P. D., Gauthier, N. C., Vonnegut, W., Mathur, A., Hone, J., Iyengar, R. and Sheetz, M. P. (2010). Cell spreading as a hydrodynamic process. *Soft Mat.* **6**, 4788-4799. doi:10.1039/c0sm00252f
- Ferreira, F., Foley, M., Cooke, A., Cunningham, M., Smith, G., Woolley, R., Henderson, G., Kelly, E., Mundell, S. and Smythe, E. (2012). Endocytosis of G protein-coupled receptors is regulated by clathrin light chain phosphorylation. *Curr. Biol.* **22**, 1361-1370. doi:10.1016/j.cub.2012.05.034
- Gaidarov, I., Santini, F., Warren, R. A. and Keen, J. H. (1999). Spatial control of coated-pit dynamics in living cells. *Nat. Cell Biol.* **1**, 1-7. doi:10.1038/8971
- Galovic, M., Xu, D., Areces, L. B., van der Kammen, R. and Innocenti, M. (2011). Interplay between N-WASP and CK2 optimizes clathrin-mediated endocytosis of EGFR. *J. Cell Sci.* **124**, 2001-2012. doi:10.1242/jcs.081182
- Gautier, J. J., Lomakina, M. E., Bouslama-Oueghlani, L., Derivery, E., Beilinson, H., Faigle, W., Loew, D., Louvard, D., Echarat, A., Alexandrova, A. Y. et al. (2011). Clathrin is required for Scar/Wave-mediated lamellipodium formation. *J. Cell Sci.* **124**, 3414-3427. doi:10.1242/jcs.081083

- Gomes, I., Sierra, S. and Devi, L. A.** (2016). Detection of receptor heteromerization using *in situ* proximity ligation assay. *Curr. Protoc. Pharmacol.* **75**, 2.16.11-12.16.31. doi:10.1002/cpph.15
- Guan, J.-L. and Shalloway, D.** (1992). Regulation of focal adhesion-associated protein tyrosine kinase by both cellular adhesion and oncogenic transformation. *Nature* **358**, 690-692. doi:10.1038/358690a0
- Harburger, D. S. and Calderwood, D. A.** (2009). Integrin signalling at a glance. *J. Cell Sci.* **122**, 159-163. doi:10.1242/jcs.018093
- Herman, I. M., Crisona, N. J. and Pollard, T. D.** (1981). Relation between cell activity and the distribution of cytoplasmic actin and myosin. *J. Cell Biol.* **90**, 84-91. doi:10.1083/jcb.90.1.84
- Hinrichsen, L., Harborth, J., Andrees, L., Weber, K. and Ungewickell, E. J.** (2003). Effect of clathrin heavy chain- and alpha-adaptin-specific small inhibitory RNAs on endocytic accessory proteins and receptor trafficking in HeLa cells. *J. Biol. Chem.* **278**, 45160-45170. doi:10.1074/jbc.M307290200
- Horn, M., Geisen, C., Cermak, L., Becker, B., Nakamura, S., Klein, C., Pagano, M. and Antebi, A.** (2014). DRE-1/FBXO11-dependent degradation of BLMP-1/BLIMP-1 governs *C. elegans* developmental timing and maturation. *Dev. Cell* **28**, 697-710. doi:10.1016/j.devcel.2014.01.028
- Huang, F., Khvorova, A., Marshall, W. and Sorkin, A.** (2004). Analysis of clathrin-mediated endocytosis of epidermal growth factor receptor by RNA interference. *J. Biol. Chem.* **279**, 16657-16661. doi:10.1074/jbc.C400046200
- Humphries, A. C. and Way, M.** (2013). The non-canonical roles of clathrin and actin in pathogen internalization, egress and spread. *Nat. Rev. Microbiol.* **11**, 551-560. doi:10.1038/nrmicro3072
- Huttenlocher, A. and Horwitz, A. R.** (2011). Integrins in cell migration. *Cold Spring Harbor Perspect. Biol.* **3**, a005074. doi:10.1101/cshperspect.a005074
- Huvneers, S. and Danen, E. H. J.** (2009). Adhesion signaling - crosstalk between integrins, Src and Rho. *J. Cell Sci.* **122**, 1059-1069. doi:10.1242/jcs.039446
- Jackson, A. P., Seow, H.-F., Holmes, N., Drickamer, K. and Parham, P.** (1987). Clathrin light chains contain brain-specific insertion sequences and a region of homology with intermediate filaments. *Nature* **326**, 154-159. doi:10.1038/326154a0
- Keen, J. H., Willingham, M. C. and Pastan, I. H.** (1979). Clathrin-coated vesicles: isolation, dissociation and factor-dependent reassociation of clathrin baskets. *Cell* **16**, 303-312. doi:10.1016/0092-8674(79)90007-2
- Kim, D.-H. and Wirtz, D.** (2013). Focal adhesion size uniquely predicts cell migration. *FASEB J.* **27**, 1351-1361. doi:10.1096/fj.12-220160
- Klumperman, J. and Raposo, G.** (2014). The complex ultrastructure of the endolysosomal system. *Cold Spring Harbor Perspect. Biol.* **6**, a016857. doi:10.1101/cshperspect.a016857
- Lawson, C. D. and Burridge, K.** (2014). The on-off relationship of Rho and Rac during integrin-mediated adhesion and cell migration. *Small GTPases* **5**, e27958. doi:10.4161/sntp.27958
- Lebensohn, A. M. and Kirschner, M. W.** (2009). Activation of the WAVE complex by coincident signals controls actin assembly. *Mol. Cell* **36**, 512-524. doi:10.1016/j.molcel.2009.10.024
- Legendre-Guillemin, V., Metzler, M., Charbonneau, M., Gan, L., Chopra, V., Philie, J., Hayden, M. R. and McPherson, P. S.** (2002). HIP1 and HIP12 display differential binding to F-actin, AP2, and clathrin. Identification of a novel interaction with clathrin light chain. *J. Biol. Chem.* **277**, 19897-19904. doi:10.1074/jbc.M112310200
- Legendre-Guillemin, V., Metzler, M., Lemaire, J.-F., Philie, J., Gan, L., Hayden, M. R. and McPherson, P. S.** (2005). Huntingtin interacting protein 1 (HIP1) regulates clathrin assembly through direct binding to the regulatory region of the clathrin light chain. *J. Biol. Chem.* **280**, 6101-6108. doi:10.1074/jbc.M408430200
- Leyton-Puig, D., Isogai, T., Argenzio, E., van den Broek, B., Klarenbeek, J., Janssen, H., Jalink, K. and Innocenti, M.** (2017). Flat clathrin lattices are dynamic actin-controlled hubs for clathrin-mediated endocytosis and signalling of specific receptors. *Nat. Commun.* **8**, 16068. doi:10.1038/ncomms16068
- Luo, Y., Zhan, Y. and Keen, J. H.** (2013). Arf6 regulation of Gyrating-clathrin. *Traffic* **14**, 97-106. doi:10.1111/tra.12014
- Machesky, L. M. and Insall, R. H.** (1998). Scar1 and the related Wiskott-Aldrich syndrome protein, WASP, regulate the actin cytoskeleton through the Arp2/3 complex. *Curr. Biol.* **8**, 1347-1356. doi:10.1016/S0960-9822(98)00015-3
- Maib, H., Ferreira, F., Vassilopoulos, S. and Smythe, E.** (2018). Cargo regulates clathrin-coated pit invagination via clathrin light chain phosphorylation. *J. Cell Biol.* **217**, 4253. doi:10.1083/jcb.201805005
- Majeed, S. R., Vasudevan, L., Chen, C. Y., Luo, Y., Torres, J. A., Evans, T. M., Sharkey, A., Foraker, A. B., Wong, N. M., Esk, C. et al.** (2014). Clathrin light chains are required for the gyrating-clathrin recycling pathway and thereby promote cell migration. *Nat. Commun.* **5**, 3891. doi:10.1038/ncomms4891
- McMahon, H. T. and Gallop, J. L.** (2005). Membrane curvature and mechanisms of dynamic cell membrane remodelling. *Nature* **438**, 590-596. doi:10.1038/nature04396
- Messa, M., Fernández-Busnadiego, R., Sun, E. W., Chen, H., Czaplá, H., Wrasman, K., Wu, Y., Ko, G., Ross, T., Wendland, B. et al.** (2014). Epsin deficiency impairs endocytosis by stalling the actin-dependent invagination of endocytic clathrin-coated pits. *Elife* **3**, e03311. doi:10.7554/eLife.03311
- Miki, H., Suetsugu, S. and Takenawa, T.** (1998). WAVE, a novel WASP-family protein involved in actin reorganization induced by Rac. *EMBO J.* **17**, 6932-6941. doi:10.1093/emboj/17.23.6932
- Morone, N., Fujiwara, T., Murase, K., Kasai, R. S., Ike, H., Yuasa, S., Usukura, J. and Kusumi, A.** (2006). Three-dimensional reconstruction of the membrane skeleton at the plasma membrane interface by electron tomography. *J. Cell Biol.* **174**, 851-862. doi:10.1083/jcb.200606007
- Nader, G. P. F., Ezratty, E. J. and Gundersen, G. G.** (2016). FAK, talin and PIPKgamma regulate endocytosed integrin activation to polarize focal adhesion assembly. *Nat. Cell Biol.* **18**, 491-503. doi:10.1038/ncb3333
- Näthke, I. S., Heuser, J., Lupas, A., Stock, J., Turck, C. W. and Brodsky, F. M.** (1992). Folding and trimerization of clathrin subunits at the triskelion hub. *Cell* **68**, 899-910. doi:10.1016/0092-8674(92)90033-9
- Palamidessi, A., Frittoli, E., Garré, M., Faretta, M., Mione, M., Testa, I., Diaspro, A., Lanzetti, L., Scita, G. and Di Fiore, P. P.** (2008). Endocytic trafficking of Rac is required for the spatial restriction of signaling in cell migration. *Cell* **134**, 135-147. doi:10.1016/j.cell.2008.05.034
- Parachoniak, C. A., Luo, Y., Abella, J. V., Keen, J. H. and Park, M.** (2011). GGA3 functions as a switch to promote Met receptor recycling, essential for sustained ERK and cell migration. *Dev. Cell* **20**, 751-763. doi:10.1016/j.devcel.2011.05.007
- Parsons, J. T., Martin, K. H., Slack, J. K., Taylor, J. M. and Weed, S. A.** (2000). Focal adhesion kinase: a regulator of focal adhesion dynamics and cell movement. *Oncogene* **19**, 5606-5613. doi:10.1038/sj.onc.1203877
- Payne, G. S. and Schekman, R.** (1985). A test of clathrin function in protein secretion and cell growth. *Science* **230**, 1009-1014. doi:10.1126/science.2865811
- Pollard, T. D. and Borisy, G. G.** (2003). Cellular motility driven by assembly and disassembly of actin filaments. *Cell* **112**, 453-465. doi:10.1016/S0092-8674(03)00120-X
- Poupon, V., Girard, M., Legendre-Guillemin, V., Thomas, S., Bourbonniere, L., Philie, J., Bright, N. A. and McPherson, P. S.** (2008). Clathrin light chains function in mannose phosphate receptor trafficking via regulation of actin assembly. *Proc. Natl. Acad. Sci. USA* **105**, 168-173. doi:10.1073/pnas.0707269105
- Price, L. S., Leng, J., Schwartz, M. A. and Bokoch, G. M.** (1998). Activation of Rac and Cdc42 by integrins mediates cell spreading. *Mol. Biol. Cell* **9**, 1863-1871. doi:10.1091/mbc.9.7.1863
- Ramirez-Santiago, G., Robles-Valero, J., Morlino, G., Cruz-Adalia, A., Pérez-Martínez, M., Zaldivar, A., Torres-Torresano, M., Chichon, F. J., Sorrentino, A., Pereira, E. et al.** (2016). Clathrin regulates lymphocyte migration by driving actin accumulation at the cellular leading edge. *Eur. J. Immunol.* **46**, 2376-2387. doi:10.1002/eji.201646291
- Rangamani, P., Fardin, M.-A., Xiong, Y., Lipshtat, A., Rossier, O., Sheetz, M. P. and Iyengar, R.** (2011). Signaling network triggers and membrane physical properties control the actin cytoskeleton-driven isotropic phase of cell spreading. *Biophys. J.* **100**, 845-857. doi:10.1016/j.bpj.2010.12.3732
- Riikonen, T., Vihinen, P., Potila, M., Rettig, W. and Heino, J.** (1995). Antibody against human alpha 1 beta 1 integrin inhibits HeLa cell adhesion to laminin and to type I, IV, and V collagens. *Biochem. Biophys. Res. Commun.* **209**, 205-212. doi:10.1006/bbrc.1995.1490
- Rizk, A., Paul, G., Incardona, P., Bugarski, M., Mansouri, M., Niemann, A., Ziegler, U., Berger, P. and Sbalzarini, I. F.** (2014). Segmentation and quantification of subcellular structures in fluorescence microscopy images using Squash. *Nat. Protoc.* **9**, 586-596. doi:10.1038/nprot.2014.037
- Royle, S. J.** (2012). The role of clathrin in mitotic spindle organisation. *J. Cell Sci.* **125**, 19-28. doi:10.1242/jcs.094607
- Royle, S. J., Bright, N. A. and Lagnado, L.** (2005). Clathrin is required for the function of the mitotic spindle. *Nature* **434**, 1152-1157. doi:10.1038/nature03502
- Schmid, S. L., Braell, W. A., Schlossman, D. M. and Rothman, J. E.** (1984). A role for clathrin light chains in the recognition of clathrin cages by 'uncoating ATPase'. *Nature* **311**, 228-231. doi:10.1038/311228a0
- Schreij, A. M., Chaineau, M., Ruan, W., Lin, S., Barker, P. A., Fon, E. A. and McPherson, P. S.** (2015). LRRK2 localizes to endosomes and interacts with clathrin-light chains to limit Rac1 activation. *EMBO Rep.* **16**, 79-86. doi:10.15252/embr.201438714
- Schreij, A. M., Fon, E. A. and McPherson, P. S.** (2016). Endocytic membrane trafficking and neurodegenerative disease. *Cell. Mol. Life Sci.* **73**, 1529-1545. doi:10.1007/s00018-015-2105-x
- Silveira, L. A., Wong, D. H., Masiarz, F. R. and Schekman, R.** (1990). Yeast clathrin has a distinctive light chain that is important for cell growth. *J. Cell Biol.* **111**, 1437-1449. doi:10.1083/jcb.111.4.1437
- Skruzny, M., Brach, T., Ciuffa, R., Rybina, S., Wachsmuth, M. and Kaksonen, M.** (2012). Molecular basis for coupling the plasma membrane to the actin cytoskeleton during clathrin-mediated endocytosis. *Proc. Natl. Acad. Sci. USA* **109**, E2533-E2542. doi:10.1073/pnas.1207011109
- Soderberg, O., Gullberg, M., Jarvius, M., Ridderstrale, K., Leuchowius, K. J., Jarvius, J., Wester, K., Hydbring, P., Bahrman, F., Larsson, L.-G. et al.** (2006). Direct observation of individual endogenous protein complexes *in situ* by proximity ligation. *Nat. Methods* **3**, 995-1000. doi:10.1038/nmeth947

- Theodosiou, M., Widmaier, M., Böttcher, R. T., Rognoni, E., Veelders, M., Bharadwaj, M., Lambacher, A., Austen, K., Müller, D. J., Zent, R. et al. (2016). Kindlin-2 cooperates with talin to activate integrins and induces cell spreading by directly binding paxillin. *Elife* **5**, e10130. doi:10.7554/eLife.10130
- Tiwari, S., Askari, J. A., Humphries, M. J. and Balleid, N. J. (2011). Divalent cations regulate the folding and activation status of integrins during their intracellular trafficking. *J. Cell Sci.* **124**, 1672-1680. doi:10.1242/jcs.084483
- Traub, L. M. and Bonifacio, J. S. (2013). Cargo recognition in clathrin-mediated endocytosis. *Cold Spring Harbor Perspect. Biol.* **5**, a016790. doi:10.1101/cshperspect.a016790
- Tsygankova, O. M., Ma, C., Tang, W., Korch, C., Feldman, M. D., Lv, Y., Brose, M. S. and Meinkoth, J. L. (2010). Downregulation of Rap1GAP in human tumor cells alters cell/matrix and cell/cell adhesion. *Mol. Cell. Biol.* **30**, 3262-3274. doi:10.1128/MCB.01345-09
- Tsygankova, O. M., Wang, H. and Meinkoth, J. L. (2013). Tumor cell migration and invasion are enhanced by depletion of Rap1 GTPase-activating protein (Rap1GAP). *J. Biol. Chem.* **288**, 24636-24646. doi:10.1074/jbc.M113.464594
- Turner, C. E. (2000). Paxillin and focal adhesion signalling. *Nat. Cell Biol.* **2**, E231. doi:10.1038/35046659
- Ungewickell, E. and Branton, D. (1981). Assembly units of clathrin coats. *Nature* **289**, 420-422. doi:10.1038/289420a0
- Ungewickell, E. and Ungewickell, H. (1991). Bovine brain clathrin light chains impede heavy chain assembly in vitro. *J. Biol. Chem.* **266**, 12710-12714.
- Wakeham, D. E., Abi-Rached, L., Towler, M. C., Wilbur, J. D., Parham, P. and Brodsky, F. M. (2005). Clathrin heavy and light chain isoforms originated by independent mechanisms of gene duplication during chordate evolution. *Proc. Natl. Acad. Sci. USA* **102**, 7209-7214. doi:10.1073/pnas.0502058102
- Wolfenson, H., Lavelin, I. and Geiger, B. (2013). Dynamic regulation of the structure and functions of integrin adhesions. *Dev. Cell* **24**, 447-458. doi:10.1016/j.devcel.2013.02.012
- Wozniak, M. A., Modzelewska, K., Kwong, L. and Keely, P. J. (2004). Focal adhesion regulation of cell behavior. *Biochim. Biophys. Acta* **1692**, 103-119. doi:10.1016/j.bbamcr.2004.04.007
- Wu, S., Majeed, S. R., Evans, T. M., Camus, M. D., Wong, N. M. L., Schollmeier, Y., Park, M., Muppidi, J. R., Reboldi, A., Parham, P. et al. (2016). Clathrin light chains' role in selective endocytosis influences antibody isotype switching. *Proc. Natl. Acad. Sci. U.S.A.* **113**, 9816-9821. doi:10.1073/pnas.1611189113
- Xiong, Y., Rangamani, P., Fardin, M.-A., Lipshtat, A., Dubin-Thaler, B., Rossier, O., Sheetz, M. P. and Iyengar, R. (2010). Mechanisms controlling cell size and shape during isotropic cell spreading. *Biophys. J.* **98**, 2136-2146. doi:10.1016/j.bpj.2010.01.059
- Yang, C., Czech, L., Gerboth, S., Kojima, S., Scita, G. and Svitkina, T. (2007). Novel roles of formin mDia2 in lamellipodia and filopodia formation in motile cells. *PLoS Biol.* **5**, e317. doi:10.1371/journal.pbio.0050317
- Zhang, X., Jiang, G., Cai, Y., Monkley, S. J., Critchley, D. R. and Sheetz, M. P. (2008). Talin depletion reveals independence of initial cell spreading from integrin activation and traction. *Nat. Cell Biol.* **10**, 1062-1068. doi:10.1038/ncb1765
- Zhao, Y. and Keen, J. H. (2008). Gyrating clathrin: highly dynamic clathrin structures involved in rapid receptor recycling. *Traffic* **9**, 2253-2264. doi:10.1111/j.1600-0854.2008.00819.x
- Zhao, Y., Gaidarov, I. and Keen, J. H. (2007). Phosphoinositide 3-kinase C2alpha links clathrin to microtubule-dependent movement. *J. Biol. Chem.* **282**, 1249-1256. doi:10.1074/jbc.M606998200